



Cite this: *Chem. Soc. Rev.*, 2025, 54, 7252

Received 2nd April 2025

DOI: 10.1039/d5cs00359h

rsc.li/chem-soc-rev

Sustainable decommissioning of perovskite solar cells: from waste to resources

Valentina Larini,[†] Matteo Degani,^{ib} Silvia Cavalli^{ib} [†] and Giulia Grancini^{ib} ^{*}

Perovskite solar cells (PSCs) have witnessed a rapid progression as emerging alternatives for innovative photovoltaics (PVs). However, this promising growth also comes with challenges related to the end-of-life (EoL) management of exhausted devices. In this review, we discuss different studies on the implications of the decommissioning of PSCs from a sustainable perspective by reviewing current PSC recycling strategies as general guidelines in the field of EoL PSCs. We hope that this review would encourage the necessary development of more virtuous energy-efficient and environmentally friendly recycling protocols for PSC recovery, from lab- to large-scale application in view of perovskite-based PV technology's imminent jump to the market.

1. Introduction

One of the most urgent global issues is accomplishing the challenge of carbon “net zero” in the context of the UN sustainable development goals. Therefore, intensifying eco-friendly energy-conversion technologies is mandatory. In this respect, the International Renewable Energy Agency (IRENA) predicted that in the coming years, photovoltaics (PVs) will lead the industry of renewable energy production. However, this inspiring near-futuristic vision comes with a downside related to the end-of-life (EoL) management of exhausted solar panels.

In fact, IRENA also estimated that global solar PV waste will reach 60 million metric tons by 2050.¹ Other studies also envision scenarios of cumulative PV module waste production between 54 million and 160 million metric tons.² Even though this may appear as a relevant quantity of waste, it is important to compare this quantity with the much higher waste production from other types of technologies (*i.e.* coal ash and oily sludge waste generated from fossil fuel energy). This means that continuous research on long-lasting high-yield PV modules together with their reuse and recycling is still of great relevance in contributing to decarbonization, and EoL strategies need to be addressed in the early stages of any solar cell technology development.

In photovoltaics, perovskite solar cells (PSCs) have attracted great attention from the scientific community and from

Department of Chemistry & INSTM, University of Pavia, Via T. Taramelli 14, 27100 Pavia, Italy. E-mail: giulia.grancini@unipv.it

[†] These authors contributed equally to the work.



Valentina Larini

Valentina Larini obtained her PhD degree in 2025, working with Prof. Giulia Grancini at the University of Pavia, Italy. Her research interest spans from device manufacturing, perovskite passivation and interface engineering to recycling of critical components of perovskite solar cells. Her enthusiasm towards business development made her to take part in the Micro, Small & Medium-sized Enterprises Day at the United Nations in 2023.



Matteo Degani

Matteo Degani is a Postdoctoral Researcher in Giulia Grancini's group at the University of Pavia, Italy. He obtained his Master's degree in Materials Science and Engineering in 2019 and his PhD degree in design and characterization of hybrid perovskite for new generation solar cells in 2023. His research interests include ad hoc interlayer fabrication and optimization to improve charge carrier collection, avoiding electron-hole recombination interfaces. He was awarded the Cariplo Research Grant 2024 for young researchers.



stakeholders and government³ as new emerging solar energy production devices⁴ owing to their various advantages. Among these, their low energy payback time (EPBT) and levelized cost of electricity (LCOE) together with a high record power conversion efficiency (PCE) make them ideal candidates in the solar arena. In less than 20 years, PSCs have approached lab-scale record efficiency (27%),⁵ which monocrystalline silicon technologies attained only after more than 50 years of research. The reason behind the success of PSCs lies in their extensive tolerance towards defects, besides being processed from solutions of the perovskite active material, which results in reduced charge carrier recombination and long carrier diffusion length, leading to remarkable PCEs.^{6,7} Perovskite materials can be integrated with other photovoltaic technologies to fabricate tandem or triple-junction solar cells, thereby exceeding the efficiency limitations of conventional single-junction devices. In the most widely studied tandem architectures, a perovskite absorber is deposited on top of another photovoltaic layer, such as a secondary perovskite layer (perovskite/perovskite) or a crystalline silicon (perovskite/silicon). Notably, in the 2-terminal perovskite/silicon configuration, recent advancements have enabled a PCE of 34.6%, demonstrating the potential of these hybrid approaches to revolutionize next-generation photovoltaics.⁸

Despite their high efficiencies and broad applicability, PSCs still suffer from device longevity with respect to the 20 years of stable operation required from commercial PV technologies.⁹ Extensive research efforts have been made to enhance the stability of PSCs,^{10,11} spanning from strategies that tackle

intrinsic properties of perovskites to encapsulation procedures to secure the device from the external environment.^{12–14} Consequently, several companies have just started working on perovskite-based PV installed pilot lines and produced module prototypes for commercialization.¹⁵ Therefore, it is estimated that perovskite-based PVs will soon contribute to the global solar PV market and consequently also to PV waste generation.

In this respect, PSC decommissioning becomes an urgent task that, in our opinion, should be readily addressed at the device design stage. According to the European Union, 80% of a product's environmental impact is determined during its design phase.¹⁶ Moreover, in line with the 12th sustainable development goal of the Agenda 2030, the recovery of PSCs would meet the requirements of responsible consumption and production patterns.¹⁷ It is also important to keep in mind that just converting renewable solar energy into electricity does not directly translate to green production. Therefore, to achieve real sustainability, both the recyclability and the environmental impact of such a novel energy-conversion technology must be considered. In this regard, the circular economy, whose pillars are, in a priority order, reduce, reuse, recycle, and recover, is the model of choice for minimizing material waste and creating further value from depleted PSCs. Life cycle assessment (LCA) comparing landfill and recycling EoL scenarios for exhausted PSCs demonstrates that the recovery of critical components of PSCs reduces the environmental impact of such technology,^{18,19} as schematically depicted in Fig. 1. Moreover, recycling PSCs results in the safe management of their toxic contents, mainly represented by lead (Pb). It is well known that Pb



Silvia Cavalli

Research Technologist, where she is currently involved in developing routes for sustainable perovskite solar cells based on green chemistry.

Silvia Cavalli obtained her Master's degree in Chemistry (2002) from the University of Milan in Italy and her PhD (2006) under the direct supervision of Prof. Dr Alexander Kros at Leiden University, The Netherlands. She has worked on different interdisciplinary projects related to the field of nanotechnology (from synthetic and physical chemistry to biology). She recently joined Prof. Giulia Grancini's group at the University of Pavia as a



Giulia Grancini

the EPFL, supported by SNSF through the Ambizione Energy Grant. Since 2019, she has been among the most highly cited scientists from the Web of Science with an h-index of 57 and more than 24 000 citations. In 2024, she was awarded the ERC Consolidator Grant "ELOW-DI" for the development of stable perovskite tandem solar cells. She also co-coordinates the EU project GoPV, a large European consortium focused on perovskite photovoltaics. She was appointed "Cavaliere della Repubblica" for scientific merit by President Mattarella. More information can be found at <https://pvsquared2.unipv.it>.

Giulia Grancini is an Associate Professor at the Chemistry Department of the University of Pavia, leading the PVsquared2 team and several international projects, such as the ERC St Grant "HYNANO" and the ERC POC "Spike", developing advanced hybrid perovskites solar cells. She obtained her PhD in Physics from Politecnico di Milano in 2012 and worked as a Postdoc Researcher at IIT in Milano. From 2015 to 2019, she was at



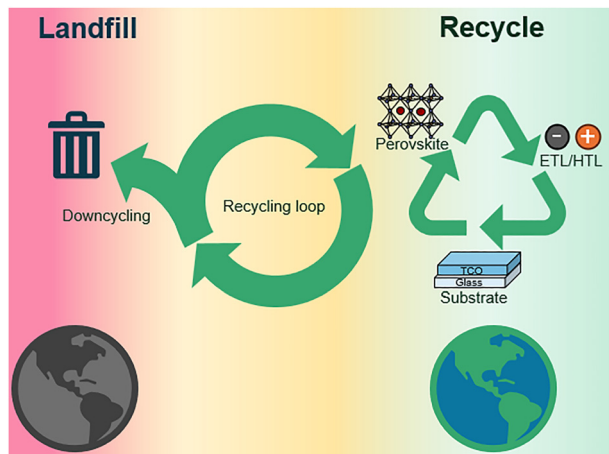


Fig. 1 Schematic of virtuous *versus* non virtuous PSC-derived waste disposal.

represents a hazard to human health because it can enter the bloodstream by several paths (ingestion, inhalation or dermal contact) and can accumulate in the skeleton (with a half-life of 40–50 years).^{20,21} Furthermore, Pb is known to be genotoxic, and it can cause neurological and non-neurological different types of disorders.²² By collecting PbI_2 or the entire perovskite from spent PSCs, lead pollution can be reduced, while PSC sustainability is enhanced.

For these reasons, in recent years, many efforts have been made to ensure the circular deployment of perovskite-based PVs, developing sustainable protocols, in particular, employing green solvents to manage EoL and remanufacturing of PSCs (e.g. recycling of toxic lead iodide component and reuse of expensive charge transporting materials and metal contacts). Meanwhile, it is compelling to adequately disseminate to the scientific community the major outcomes of this important research aspect to boost perovskite-based PV technology's full development and its imminent launch to the market.

Thus, in this review, we first give a brief introduction to PSC technology, mainly focusing on the architecture of the different available devices, as basic knowledge to allow full comprehension of the subject to non-specialised readers. Then, we present various studies on the implications of the decommissioning of PSCs from a sustainable perspective through an overview of the proposed LCA and techno-economic analysis (TEA) in the literature, demonstrating the fact that such types of environmentally friendly “best practices” applied to PSCs can produce valuable resources from waste even at the lab-scale. We further proceed by commenting on different recovery protocols by discussing several published works from lab- to large-scale. Specifically, we summarise the existing recovery strategies for each (or multiple) material(s) that comprises PSCs, providing an overview of related articles following the waste hierarchy reported in the Directive 2008/98/EC of the European Parliament. Then, we discuss the impact of the solvent choice on recycling strategies and the rationale behind its selection, with special attention paid to the implementation of the use of green

solvents. Finally, we conclude by summarising the main outcomes as general guidelines in the field and providing future perspectives.

2. Perovskite photovoltaic technologies

Perovskites are a class of materials characterized by an ABX_3 crystal structure, where “A” represents an organic or inorganic cation, such as cesium (Cs^+), methylammonium (MA^+ , CH_3NH_3^+), and formamidinium (FA^+ , $\text{CH}_3\text{CH}_2\text{NH}_3^+$). The “B” site is occupied by a metal cation, commonly tin (Sn^{2+}) or lead (Pb^{2+}), while “X” is a halide anion, including iodide (I^-), chloride (Cl^-), or bromide (Br^-). By carefully selecting different combinations of these elements, it is possible to tailor the properties of perovskite materials for specific applications in photovoltaics and optoelectronics.^{4,23,24}

One of the key advantages of lead-based perovskite materials is their excellent optoelectronic properties. They exhibit a high absorption coefficient ($\sim 5.7 \times 10^4 \text{ cm}^{-1}$ at 600 nm), low Auger recombination, efficient charge carrier mobility ($1\text{--}10 \text{ cm}^2 \text{ V}^{-1} \text{ s}^{-1}$), and long charge diffusion lengths. These characteristics make perovskites highly attractive for applications in solar cells, light-emitting diodes (LEDs), photodetectors, and other optoelectronic devices.

Furthermore, tunable bandgaps ranging from 1.3 to 2.2 eV are extremely important for tandem and multi-junction solar cells (Fig. 2c and d).²⁵ In fact, in the context of perovskite solar cells (PSCs), different device architectures can be employed.²⁶ As schematically illustrated in Fig. 2a and b, the single-junction

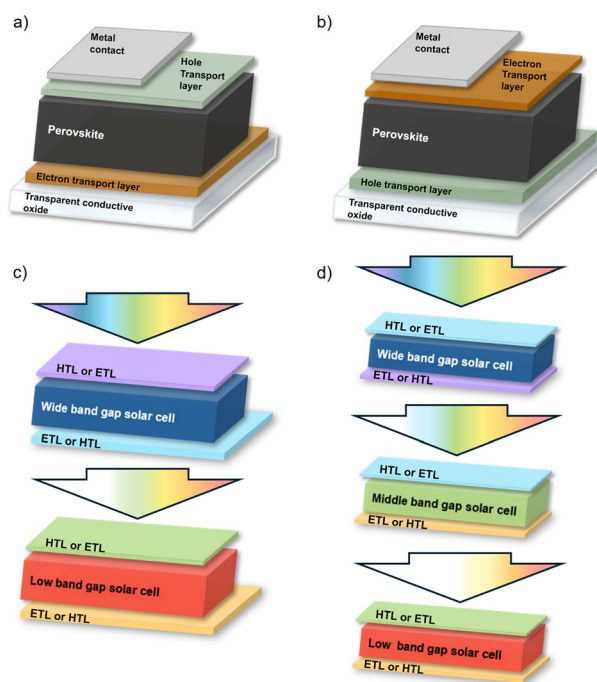


Fig. 2 Schematic illustration of different perovskite device architectures: (a) NIP, (b) PIN, (c) tandem and (d) triple junction solar cells.



configuration follows either an n-i-p (NIP) or p-i-n (PIN) structure depending on the arrangement of the charge transport layers relative to the light path.²⁷ Common hole transport materials (HTMs) include spiro-OMeTAD, NiO, PTAA, and SAM layers, while electron transport materials (ETMs) frequently used are C₆₀, PCBM, and SnO₂.^{28,29}

Perovskite materials offer versatile applicability across various photovoltaic (PV) domains,³⁰ including indoor PV, building-integrated photovoltaics (BIPV), and agrivoltaics.^{31,32} This broad adaptability stems from their facile processability, as perovskite films can be deposited using solution-based techniques or vacuum evaporation methods, enabling scalable and cost-effective manufacturing.³³

3. Sustainability and economic considerations of decommissioning PSCs

From an eco-friendly broad context, green energy production plays a strong role in fighting the climate crisis, with the ambition of substituting fossil fuels with other renewable sources of energy. The selection of one type over another technology can be driven by several aspects, such as geographical collocation and material availability. For a total evaluation of new green energy-conversion technology, besides efficiency, lifetime, and ease of manufacturing, environmental sustainability and economic advantages are timely fundamental aspects to consider when developing novel techniques and must also be considered as important indicators when designing proper recovery strategies. In fact, each adopted process accounts for material and electricity consumption as well as for environmental impact, which needs to be carefully evaluated to render both the process and the recovery protocols advantageous from a commercialisation perspective. LCA and TEA have been performed to evaluate the competitiveness of different PV technologies³⁴ and can also be useful types of studies to compare different recoveries of PV device processes.

In the context of perovskite-based PVs, works that compare circular EoL approaches with landfill EoL scenarios for PSCs are of fundamental importance to foresee a virtuous direction to sustainable PSC commercialisation that may start already at the lab-scale and are discussed in detail in the subsequent sections.³⁵

3.1. Environmental impact of recovery strategies by life cycle assessment

As anticipated above, LCA is a powerful tool for assessing the environmental impact of a product. Usually performed as a comparative analysis, it evaluates the sustainability of all manufacturing, operational, and disposal processes occurring during a product's lifetime. Although some studies performed a comparative LCA to estimate the profitability of PSCs with respect to other PV technologies,^{36–38} other types of studies evaluated the effects of PSC recovery as opposed to landfilling.^{18,39} In this respect, the effect of material recovery on

Table 1 Comparison of EPBT and LCOE of PSC and Si PV technologies

	PSCs	Si PVs
EPBT (years)	0.19–0.60	1.3–2.4
LCOE (€cents per kW h)	Estimated 4.52–6.11	4.1–9.2

primary energy consumption (PEC), global warming potential (GWP), energy payback time (EPBT), and greenhouse gas (GHG) emissions are several environmental-related indicators to consider in an LCA analysis.

Tian *et al.*¹⁸ performed an LCA on six PSC architectures and identified the most advantageous device stacks by considering several environmental-related indicators. As shown in Table 1, PSCs can be fully competitive with their silicon counterparts. According to the study, the EPBT for silicon photovoltaics is approximately 2.4 years under a landfill end-of-life scenario, which can be reduced to 1.3 years when recycling processes are implemented. In comparison, PSCs exhibit significantly shorter EPBT values in all analysed cases, ranging from 0.19 to 0.60 years under landfill conditions, with further reductions anticipated under recycling scenarios. Although some uncertainty remains regarding the precise LCOE values for perovskite technology, a reliable estimate ranges from 4.52 to 6.11 €cent per kW h, demonstrating cost competitiveness with silicon-based photovoltaics.⁴⁰

Results showed that in all cases, the recovery of critical components of PSCs can reduce the environmental footprint of the technology (Fig. 3).

Similarly, in a recent work conducted by our group, we developed a circular recovery method to reuse and recycle key PSC materials and performed an LCA to assess its profitability with respect to a landfill end-of-life scenario. The analysis of full-spectrum midpoint impact categories revealed that the application of our circular recovery approach is definitively more beneficial with respect to the landfill EoL scenario.⁴¹ Finally, Rodríguez-García *et al.*⁴² analysed 13 PSC recycling techniques reported in the literature that focused on transparent conductive oxide (TCO)-coated glass recovery. Surprisingly, their comparative LCA revealed that all considered processes, except for one, generated a higher environmental impact than the production of virgin substrates. In particular, the highest footprint was generated by chemicals used to dissolve the PV layers of the stack. Dimethylformamide (DMF), a toxic and environmentally harmful solvent,^{43,44} was employed in most of the impactful techniques analysed, while potassium hydroxide (KOH) aqueous solution was used in the process that truly resulted in a sustainable one. We can therefore conclude that the choice for using “greener” solvents, which is extensively discussed later in this review in a dedicated section, seems to be crucial in reducing the environmental impact of PSC recovery protocols.

3.2. Impact of recovery strategies on costs by techno-economic analysis

In a similar manner to LCA, TEA can be performed to estimate the economic profitability of a product in comparison to others, considering all lifetime stages, from production to disposal.



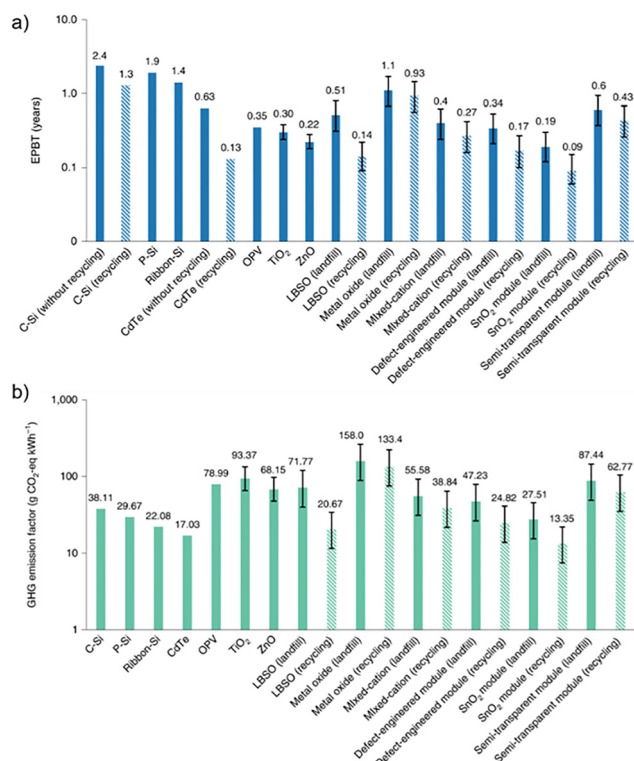


Fig. 3 Comparison of (a) EPBT and (b) GHG emission factors among 13 PV modules based on different technologies. The solid bars correspond to landfill end-of-life scenarios for different PV modules, while the striped bars correspond to the recycling counterparts. The evaluations are based on rooftop-mounted installation in Southern Europe, with annual irradiation of 1700 kW h m⁻² and a performance ratio of 75%. Error bars, 95% confidence intervals. Reproduced with permission.¹⁸ Copyright 2021, Nature.

The LCOE is a common indicator that allows for the calculation of the average cost of electricity in a currency per energy unit and can help assess the electricity generation costs of a technological process. Similarly, the minimum sustainable price (MSP) can be an important indicator to consider for providing the minimum rate of return (*i.e.* the efficiency of a technology in generating profits in relation to the resources used) necessary for a given industrial process to support a sustainable business over the long term.

Since most TEA studies on perovskite-based PVs neglect EoL impact, Martulli *et al.*³⁹ proposed a model that considers both financial and environmental key indicators to obtain a complete environmental-techno-economic assessment (ETEA), evaluating the restoration of PSCs from an LCA perspective and estimating its economic advantages. Their study assessed the effects of different levels of recovery rates and retained PSC performance on device sustainability. The work also demonstrated that EPBT and GHG emission factors of PSCs can be decreased up to 23% and 13%, respectively, when high levels of recovery (> 90%) and slightly reduced efficiency are achieved. Moreover, they calculated that the MSP and LCOE of PSCs can be reduced by 14% and 4%, respectively, if PSCs were recovered with high recovery levels (~100%) and no performance loss.

Wu *et al.*⁴⁵ compared the manufacturing costs of 1 m² PSC fabricated with either fresh or recovered components. Their study reveals that the reuse of substrates and the recycling of the perovskite layer and HTL would reduce costs by 63.7% and 90.7% for devices fabricated at laboratory and industrial scales, respectively.

McGovern *et al.*⁴⁶ presented a techno-economic study of perovskite PV technologies, comparing rigid and flexible single-junction perovskite modules to crystalline silicon PV (Si PV). They calculated the LCOE as a function of module efficiency and stability for a set of four modules. The LCOE equation demonstrated that low-weight flexible perovskite modules are promising. In fact, even though they are only slightly more interesting than rigid perovskite modules in competing against the Si PV utility sector, LCOE greatly benefited when considering the production of flexible low-weight modules by roll-to-roll manufacturing. Furthermore, LCA was performed for a representative flexible PSC device with 14% power conversion to evaluate the environmental impact of each layer in the flexible PSC architecture.

This type of comparison is important because flexible perovskite PVs can, in principle, broaden the range of PV applications, reaching novel PV market areas that are currently not achievable by exploiting both rigid perovskite and Si PVs.⁴⁷

4. End-of-life management of perovskite solar cells

Considering the rapid growth in photovoltaic technology, circular recycling is trivial in PV deployment. Therefore, addressing the potential accumulation of large amounts of discarded solar panels is increasingly relevant for developing the sustainable decommissioning processes of photovoltaics. Presently, the recycling of commercial silicon PV modules is quite challenging owing to laborious component separation, leading to downcycling.⁴⁸ In contrast, layer-by-layer PV devices, such as PSCs, could potentially allow for a relatively easy separation of material components through a selective dissolution strategy.⁴⁹ Even though the perovskite PV device commercialisation process is still in its infancy,¹⁵ we believe that the intrinsic potential impact on recycling of such a type of device should already be addressed at the developing stage of this technology to pave the way towards fully sustainable PSCs.

As extensively demonstrated in the previous section of this review, TEA and LCA confirmed the economic benefits of developing recycling procedures that can reduce environmental impacts at both the laboratory and industrial scales.

To program proper decommissioning strategies as a first step, it is important to identify the most critical components of PSCs. Once spotted, it is key to define directives for the design of dismissal processes. Fig. 4 presents a schematic representation of the waste hierarchy pyramid reported in the Directive 2008/98/EC of the European Parliament, where waste avoidance and waste treatment strategies are arranged from the most preferred (at the top) to the least preferred (at the bottom).⁵⁰



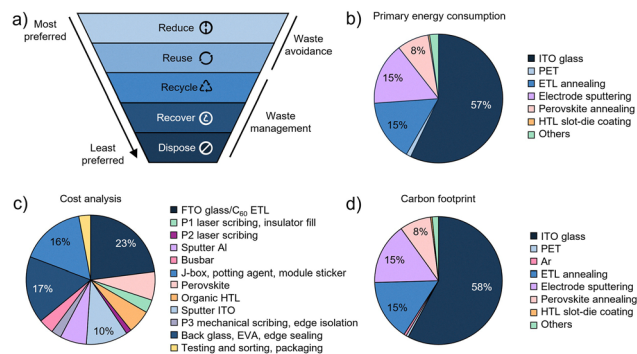


Fig. 4 (a) Waste hierarchy pyramid as reported in the Directive 2008/98/EC of the European Parliament and of the Council of 19 November 2008 on waste and repealing certain directives.⁵⁰ Analysis of the (b) primary energy consumption, (c) cost analysis and (d) carbon footprint of perovskite solar cells.

When possible, reduction and reuse are to be pursued since they completely avoid waste generation. Recycling and recovery, instead, must be put in place before disposal when waste avoidance is impossible.

In this section, we summarise the existing recovery strategies for each (or multiple) material(s) that comprise PSCs, providing an overview of related articles following the waste hierarchy pyramid.

4.1. Evaluation of the economic and environmental impact of each perovskite solar cell component

The rational design of recovery strategies for PSCs involves determining the economic and environmental impact of each component of the technology. Through such analyses, materials can be ranked in terms of cost and sustainability, and their recovery urgency can be estimated. In Fig. 4b–d, the analysis of the primary energy consumption, costs and carbon footprint considering each perovskite solar cell component is graphically presented.

Nazeeruddin and coworkers⁵¹ performed a cost analysis to produce perovskite solar panels. In their analysis, the material and equipment costs associated with perovskite PV production were estimated by comparing the impact of selecting different ETL and electrode materials in multiple locations. Significant variance was found in all metrics between the selected locations, which were considerably affected by local glass processing prices. Furthermore, in one of our studies,⁵² it emerged that transparent conductive oxide (TCO) glass coated with an electron transport layer (ETL) outweighs all other constituents, clearly indicating its high impact on manufacturing costs (23% of the cost analysis; pie chart depicted in Fig. 4c).

Furthermore, from an environmental footprint perspective, in the LCA proposed by Tian *et al.*¹⁸ mentioned in Section 3.1, the contribution that each component of the device has on its carbon footprint and PEC is evaluated, considering six different single-junction perovskite solar module (PSM) architectures. From an embedded material perspective, transparent conductive oxide (TCO)-coated glasses, such as indium tin oxide (ITO)

and fluorine tin oxide (FTO), are widely used in solar cells owing to their excellent electrical conductivity and optical transparency, representing the most environmentally impacting component for all PSM architectures. Regarding manufacturing processes, although different architectures were characterized by different fabrication processes, those that required high temperatures or energy-intensive procedures were generally marked by higher PEC and carbon footprints.

Wu *et al.*⁴⁵ demonstrated the high economic impact of the TCO glass, estimating the mass and cost composition of a 1 m² PSM based on indium tin oxide (ITO)/tin oxide (SnO₂)/methylammonium lead iodide (MAPbI₃)/N²,N^{2'},N⁷,N^{7'}-tetrakis(2,4-dimethoxyphenyl)-N²,N^{2'},N⁷,N^{7'}-tetraphenyl-9,9'-spirobifluorene]-2,2',7,7'-tetraamine (spiroOMeTAD)/Au. The ITO-coated substrate comprised almost the entire total mass (99.9%) and most of the total cost (58.3%) of the device. Furthermore, in 2020, NREL conducted a TEA, where manufacturing costs were estimated for a sheet-to-sheet single junction PSM produced in the United States.⁵³ The analysis considered all steps of module production and installation, evaluating material cost, labour, utilities, maintenance, and depreciation. Thus, TCO was the most impacting component from both economic and environmental perspectives.

It is important to keep in mind different types of PSCs such as flexible PSC devices that employ alternative materials as substrates, such as plastic-based ITO using polyethylene terephthalate (PET) and polyethylene naphthalate (PEN), for which it is important to estimate costs and plan targeted recovery or recycling protocols. Even though the estimated costs of PET and PEN are lower than those of glass, they have petrochemical origins. Hence, their use may be associated with environmental pollution issues that need to be addressed differently from glass when considering their EoL management.⁵⁴

Furthermore, the second highest GWP is the back glass used for encapsulating the device. Bogachuk *et al.*⁵⁵ developed a novel thermally assisted mechanochemical approach to remove it along with most of the device constituents for remanufacturing PSCs. From a production perspective, it is therefore important to lower fabrication costs by developing highly effective and low-cost encapsulation materials as well as low-cost materials for charge transport layers and electrodes.⁵⁶

Moreover, other impacting components are the metal contacts of PSCs. Industrial-scale PSC manufacturing is envisioned to also adopt different materials for metal contact (*i.e.* carbon) and different deposition methods that require additional recovery studies. For instance, Li. G *et al.*⁵⁷ recently published a material cost analysis in which the costs of NIP and PIN PSCs were highly comparable (\$86.49 and \$81.31, respectively), while costs significantly reduced to \$41.16 for carbon devices (49–52% reduction). This result is related to the fact that a carbon electrode is much cheaper than any noble metal electrode. Moreover, for carbon electrode deposition, a slot-die coating process associated with low energy consumption is needed. On the contrary, the deposition of noble metals requires an expensive physical vapor deposition process with high energy consumption. From a circular EoL management perspective,



the reuse of collected metal contacts from spent devices is also an important aspect to consider, which is, however, still challenging. Many studies have described protocols for metal contact collection but do not reuse them in refabricated PSCs.⁵⁸ This is related to the constraints that lab-scale fabrication imposes on metal contact deposition, which is usually performed by thermal evaporation and on metal contact choice, usually Au or Ag.

Cordell and coworkers⁵⁹ presented a recent cost analysis of perovskite/silicon (Si) tandem modules with an efficiency of 25% and found that the choice of Si cell architecture, overall module efficiency, and factory throughput have the most significant impact on cost and competitiveness. In fact, they calculated an MSP of \$0.428/WDC for their baseline two-terminal design and \$0.423/WDC for their baseline four-terminal design, each at a module production of 3 GW per year in the United States.

Besides, considering all aspects previously mentioned in the introduction, the toxicity of Pb and the instability of perovskites prevent us from ignoring the threat that Pb-based PSCs might pose to the environment and human health. Several studies have demonstrated that when Pb enters the soil, it can be easily absorbed by plants⁶⁰ and, if present in water, it can accumulate in aquatic animals,⁶¹ thus entering the food chain. In humans, Pb can enter the bloodstream by ingestion through intestinal absorption, inhalation or skin contact.⁶² It can then accumulate in organs and the skeleton and impair physiological functions and biochemical processes by mimicking biological ions such as Ca^{2+} , Fe^{2+} and Zn^{2+} .⁶³ This issue results in neurotoxicity, detrimental effects on renal function and immunity, heart diseases and carcinogenicity.^{62,63} Zhang *et al.*⁶² calculated that even low fractions of Pb leaking from the PSCs into the food chain would exceed the threshold of the Pb weekly intake limit set by the Food and Agriculture Organization (FAO) of the United Nations.

In this respect, the issue related to Pb management has been addressed in several ways, such as by using lead-free perovskites (*i.e.* tin-based PSCs).⁶⁴ However, so far, this alternative strategy has not yet proved sufficiently valid owing to the poor stability and low efficiency of these types of devices. Moreover, PbI_2 sequestration using passivation or device encapsulation is a different attempted strategy for reducing the risks related to Pb use.³⁰ Furthermore, Pb recycling is indeed an alternative strategy to mitigate its long-term risk. In fact, from a recovery perspective, the safe manipulation of EoL PSCs could contribute to the prevention of Pb pollution, complementing other practices and easing the way toward PSC commercialization.

Once the most impacting components are spotted, it is essential to define the directives for the disposing processes following the waste hierarchy.

4.2. Highest priority in the waste hierarchy: material reuse

As the most impacting components from both economic and environmental perspectives, extensive studies have been conducted to design the recovery of TCOs. Their reuse is made possible by the superior adhesion that exists between glass and TCO, which is derived from the commonly employed TCO

deposition technique of magnetron sputtering. TCOs are usually exposed from spent PSCs by dissolution with the proper solvents of the upper layers of the stack and are then subjected to standard cleaning steps. They can be restored from both single- and multi-junction solar cells, and, in some cases, charge transport materials (CTMs) can be recovered together with the TCO substrate.

4.2.1. Transparent conductive oxide reuse. The reuse of TCO substrates can be achieved when all the other layers of the PSCs are soluble in proper solvents or can be physically removed without compromising the TCO quality.

For instance, fluorine-doped indium tin oxide (FTO) substrates were successfully restored by Chowdhury *et al.*⁶⁵ and Huang *et al.*⁶⁶ through the dissolution of the above layers with DMF. The as-obtained FTO glasses displayed similar crystallinity, optical and morphological properties with respect to pristine samples. Furthermore, Huang *et al.*⁶⁶ demonstrated that the reuse of the FTO substrate does not affect the properties of the freshly deposited perovskite, thus enabling the fabrication of PSCs with performances similar to those produced with pristine substrates. Augustine *et al.*⁶⁷ achieved similar results by employing a KOH solution in deionized water ($\text{DI H}_2\text{O}$), instead of DMF, for the dissolution of the device components. Substrates refurbished with this strategy presented similar transmittance, conductivity, and roughness to pristine samples and a high degree of purity. Despite some K traces persisting on the surface of the recovered substrates, the performance of the refabricated PSCs was higher than those of fresh devices owing to the improved wettability that such K species conferred to the restored ITO surface. The recovery of the ITO glass substrate was also demonstrated for a perovskite-perovskite tandem solar cell and was hypothesized for a perovskite-silicon tandem by Tian *et al.*¹⁹ (Fig. 5a and b). First, device active layers were removed through subsequent cleaning steps in an aqueous cleaning solution, $\text{DI H}_2\text{O}$, acetone and isopropyl alcohol (IPA). Then, the effectiveness of the recovery protocol was tested by comparing the PCE of perovskite-perovskite tandems fabricated with pristine and recovered ITO substrates. Solar cells fabricated with restored ITO glass demonstrated a higher efficiency of 22.2% (20.8% on average) with respect to the pristine substrate (21.7% for the champion device, 20.3% on average), which progressively increased after each recycling iteration, reaching a champion of 22.9% (21.4% on average) (Fig. 5c and d).

4.2.2. Restoration of metal oxide-coated transparent conductive oxide. In some cases, TCO reuse cannot be decoupled from the recovery of CTMs coated on top. This is particularly true when the CTM is a metal oxide that remains firmly attached to the TCO surface, even upon solvent treatment. Therefore, several metal oxides, either used as ETL or HTL, have been recovered together with the TCO.

Feng *et al.*⁶⁸ tested several dialkylamines to recover NiO_x HTL-coated ITO substrates and ultimately selected a butylamine (BA):dipropylamine (DPA)-based 2-step approach. The improved PCE displayed by PSCs fabricated with restored substrates ($18.65 \pm 0.6\%$ with respect to the pristine device,



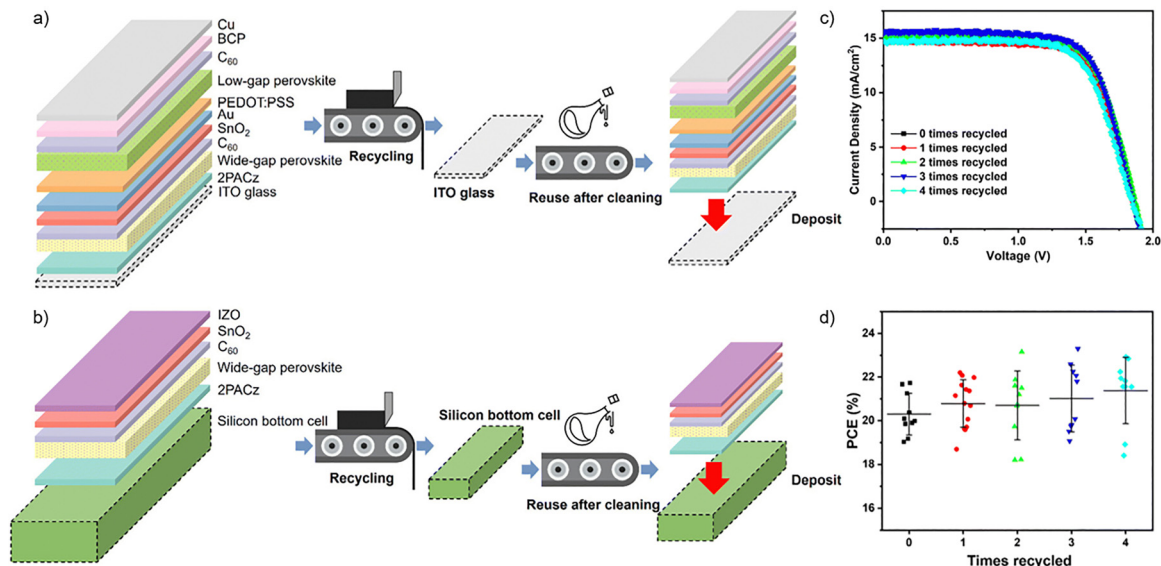


Fig. 5 Scheme of the recovery route for (a) ITO glass substrates constituting a perovskite–perovskite tandem solar cell and (b) silicon bottom cell constituting a perovskite–silicon tandem solar cell. (c) J–V curves and (d) PCE statistical analysis of the perovskite–perovskite tandem solar cell fabricated with ITO glass substrate recovered zero to four times. Reproduced with permission.¹⁹ Copyright 2023, the Royal Society of Chemistry.

16.46 \pm 0.6%) was attributed to the ability of alkylamines to template the growth of high-quality perovskites and passivate the HTL/perovskite interface. Similarly, Zhu *et al.*⁶⁹ fabricated PSCs that displayed higher PCE when refurbished substrates were employed. They noticed that the refurbished FTO/titanium oxide (TiO_2) substrate contained high quantities of Ti^{3+} ions and some residual perovskite with a Pb-rich composition. The authors correlated the presence of these species to work function

reduction and the conduction band minimum (CBM) narrowing. Although the former promoted electron–hole pair separation and suppressed recombination of charge carriers, the latter reduced interfacial recombination, ultimately leading to higher PCE. In a recent study, our group reported an enhancement of the average PCE upon the restoration of the SnO_2 ETL-coated ITO by employing DMSO (and DMF for comparison) to dissolve the upper layers of the device (Fig. 6a–c).⁵² In this case, the efficiency improvement

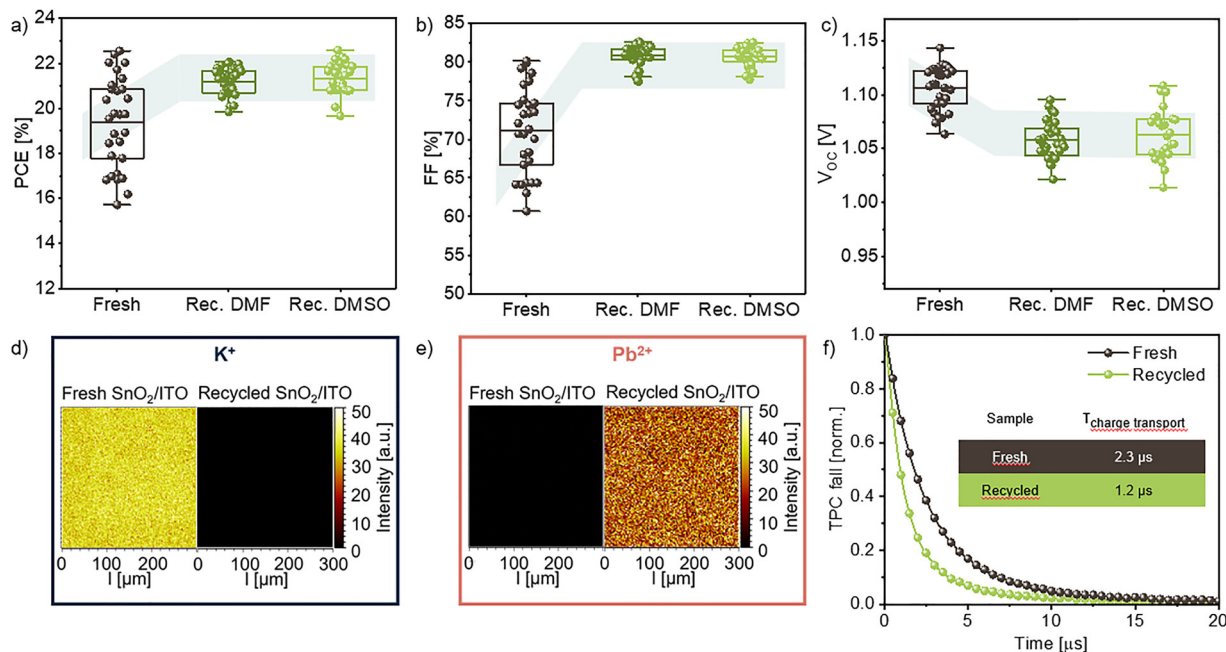


Fig. 6 (a) PCE, (b) FF and (c) V_{OC} box charts of PSCs fabricated with fresh and recycled SnO_2 /ITO glass substrates. Time of flight–secondary ion mass spectroscopy (ToF-SIMS) (d) K^+ and (e) Pb^{2+} surface maps of fresh and recycled SnO_2 /ITO glass substrates. (f) Transient photocurrent (TPC) decay curves of fresh and recycled SnO_2 /ITO glass substrates. Reproduced with permission.⁵² Copyright 2023, Wiley.



was strictly related to an average fill factor (FF) enhancement, which counterbalanced a slight open-circuit voltage (V_{OC}) reduction (Fig. 6d and f). Although the average V_{OC} decrease upon substrate restoration was correlated with the removal of K^+ ions from the surface of ITO/SnO₂, inducing higher charge-carrier recombination, the average FF increase was ascribed to the effect of PbI₂ residuals on the surface of restored substrates. With a wider bandgap than the perovskite, PbI₂ can trap holes generated in the ETL, preventing recombination at the ETL/perovskite interface and facilitating charge extraction, as suggested by transient photocurrent measurements (Fig. 6f). In contrast, although Kim *et al.*⁷⁰ observed the presence of residual chemical species on the surface of restored FTO/mesoporous (mp)-TiO₂ substrates, they did not witness an enhancement in the PV performance of their recovered PSCs. The morphological, structural and optical properties of refurbished substrates remained unchanged with respect to pristine samples, leading to almost the same efficiency of fresh devices, with minor PCE losses after iterating ten times the recovery process.

4.2.3. Restoration of transparent conductive oxide coated with mesoporous structures. The restoration of TCO substrates from PSCs with mesoporous configurations has been similarly demonstrated. In this case, the use of proper solvents leads to the removal of the perovskite layer from the device structure. Once the TCO/CTM substrate is restored, the perovskite can be reloaded into the mesoporous scaffold to produce recovered devices.

Huang *et al.*⁷¹ demonstrated the reuse of both FTO/compact (c)-TiO₂ and FTO/c-TiO₂/mp-TiO₂ substrates. After the dissolution of HTL and perovskite with DMF, both types of restored substrates displayed similar morphology and composition to the pristine samples. To further demonstrate the efficacy of the recovery process, a fresh perovskite was coated onto fresh and refurbished substrates, and its optical, structural and morphological properties were investigated. Ultimately, PSCs were fabricated by employing fresh and restored FTO/(c)-TiO₂ and FTO/c-TiO₂/mp-TiO₂, which retained 90% and 85% of the original PCE, respectively, and 84% and 74% of the original PCE, respectively, after one additional recovery iteration. Types of mesoporous scaffolds other than mp-TiO₂ have also been explored. Zhao *et al.*⁷² adopted super-aligned zinc oxide (ZnO) nanorods as mesostructured ETM; Ku *et al.*⁷³ employed an mp-Ni counter electrode coated onto an FTO/TiO₂/aluminum oxide (Al₂O₃) substrate, and Li *et al.*⁷⁴ designed an FTO/mp-TiO₂/mp-Al₂O₃/nanoporous (np)-Au:NiO_x template. These three studies feature the dissolution of the perovskite with DMF and its reloading to fabricate refurbished PSCs. Bogachuk *et al.*⁷⁵ went one step further, recovering not only the FTO-glass substrate coated with c-TiO₂/mp-TiO₂/mp-zirconium oxide (ZrO₂) from a carbon-based PSM but also the back glass used for encapsulating the device, which is the component with the second highest GWP. The FTO substrate and the back sheet were manually separated after thermal treatment at 120–140 °C. The back glass was cleaned from polyisobutylene (PIB) and thermoplastic polyolefin (TPO) by peeling off after 1 hour in acetone. The FTO glass (10 × 10 cm² plates) was restored by removing the

perovskite in a bath of methylamine and ethanol (EtOH), followed by annealing at 400 °C. Finally, the encapsulated PSCs were refabricated, showing 88% of the original PCE. Interestingly, Kadro *et al.*⁷⁶ envisioned the recovery of all components of an NIP by selectively dissolving all layers of the device. Although the fate of HTL, PbI₂ and Au was discussed, only the FTO/mp-TiO₂ substrate was eventually recovered. Refabricated PSCs retained the same PCE as fresh devices, even after the second recovery iteration of the TCO/ETL.

4.2.4. Reuse of silicon sub-cells. Although Si exhibits different chemical, morphological, and electrical properties than TCOs, a recovery strategy similar to those previously mentioned was adopted by Yang *et al.*⁷⁷ to restore the Si bottom cell of a perovskite–Si tandem solar cell. First, glass–glass encapsulation was removed by thermal delamination. Then, the perovskite top cell was dissolved in a DMF:DMSO = 4:1 mixture, and the poly(bis(4-phenyl)(2,4,6-trimethylphenyl)amine (PTAA) HTL was removed with toluene (Fig. 7a). The recollected double-sided textured Si wafer was subjected to optical (Fig. 7b), morphological (Fig. 7c and d) and PV (Fig. 7e) investigations to ensure the preservation of its properties. When the refurbished Si bottom cell was employed to fabricate new perovskite–Si tandem devices, 98% of the original average efficiency was preserved, with a champion of 25.7% PCE (Fig. 7f and g).

4.3. Middle priority in the waste hierarchy: material recycling

According to the waste hierarchy, when the reuse of components is impossible, material recycling must be pursued. Regarding PSCs, critical materials other than the TCO, such as toxic PbI₂ and some expensive CTMs, cannot be reused without any additional treatment and their recovery needs to go through some recycling steps. The recycling of costly CTMs, such as spiro-OMeTAD, is usually presented in the literature as part of more comprehensive recovery routes, where several device components are simultaneously recycled and reused. Thus, strategies addressing their recycling will be presented later in the section dedicated to the reuse and recycling of full device components. The first part of the section focuses on PbI₂ recycling, for which various methods have been proposed, all aimed at reducing the risks associated with EoL management.

4.3.1. Adsorption or complexation of lead iodide. Among several methods for recycling PbI₂, its adsorption or complexation, followed by its release in the form of PbI₂, has been broadly studied.

Yang *et al.*⁷⁸ employed a supramolecular complexation method based on chemical coordination and multidentate chelation between 2-hydroxypropyl-β-cyclodextrin (HPβCD)-1,2,3,4-butane tetracarboxylic acid (BTCA) complex and Pb²⁺ ions (Fig. 8a). HPβCD-BTCA complex was integrated into PSCs as a built-in network embedded in the active layer, and its Pb²⁺ sequestration capability was tested by subjecting damaged encapsulated devices to continuous water scouring for 1 h. The pristine sample showed a Pb leaking rate of 973 mg m⁻² h⁻², while the complex-containing sample displayed a leaking rate of 54 mg m⁻² h⁻² (Fig. 8b), which was further reduced to 14 mg m⁻² h⁻² (corresponding to 98.6% of Pb sequestration efficiency) when the



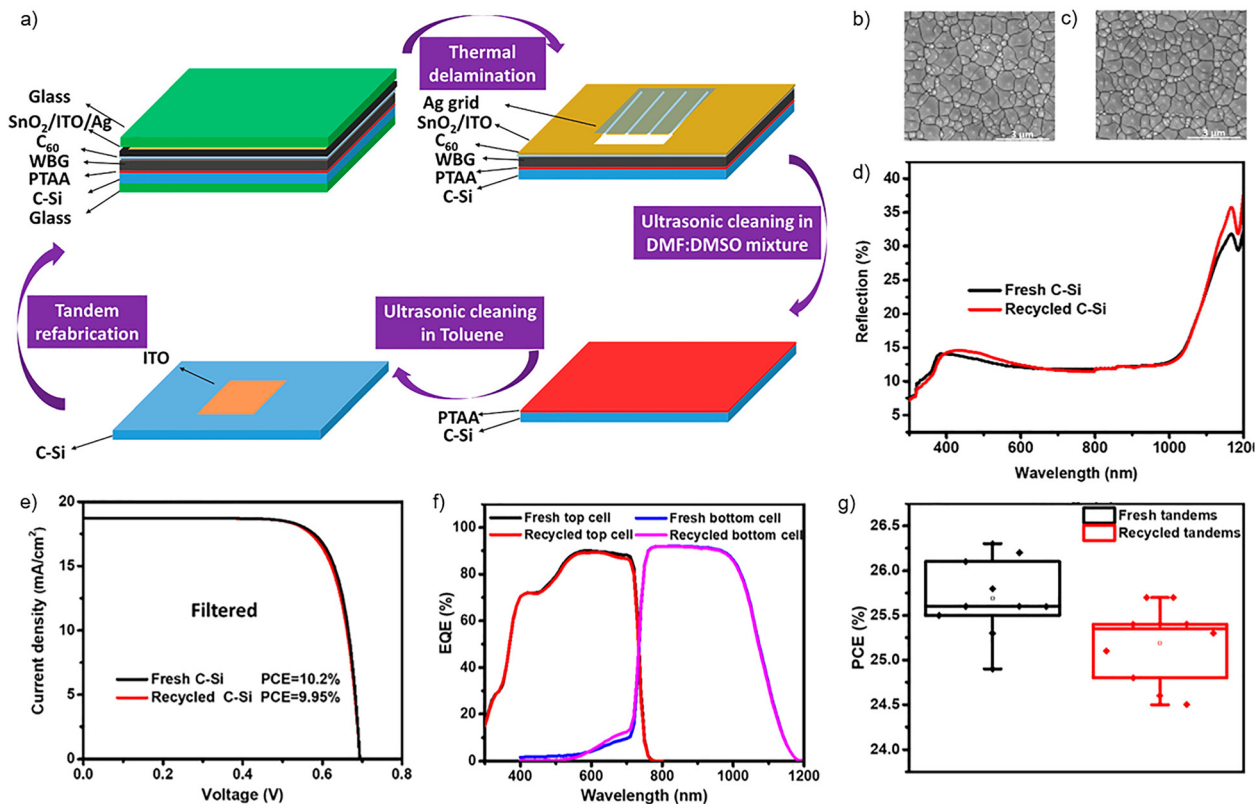


Fig. 7 (a) Schematic recycling process of Si bottom cells from degraded, encapsulated perovskite-Si tandem solar cells. Top-view SEM images of (b) fresh and (c) recycled Si bottom cells. (d) Reflectance spectra of fresh and recycled Si bottom cells. (e) J - V curves of the recycled single-junction silicon bottom cells. (f) EQE spectra and (g) PCE box charts of fresh and refabricated tandem devices. Reproduced with permission.⁷⁷ Copyright 2023, the American Chemical Society.

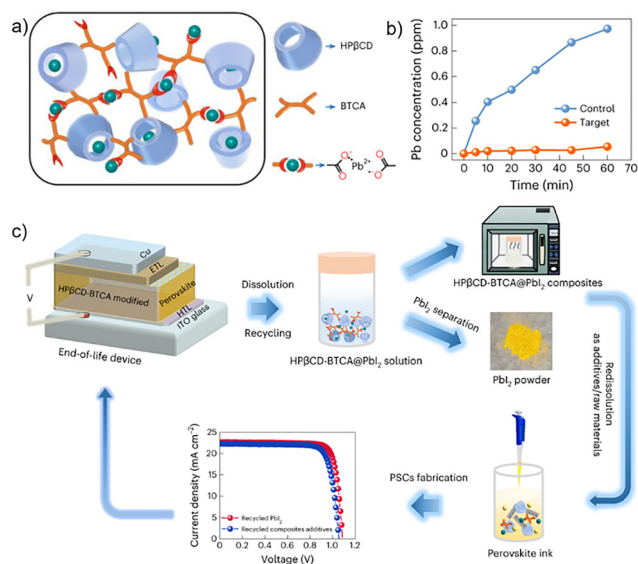
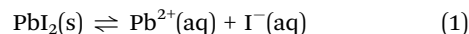


Fig. 8 (a) Schematic of lead capturing by cross-linking HPβCD-BTCA supramolecular complex. (b) Comparison of Pb sequestration for the damaged PSCs with or without HPβCD-BTCA. (c) Illustration of the process of Pb recycling and management in PSCs. Reproduced with permission.⁷⁸ Copyright 2023, Nature Publishing Group.

encapsulating cover glass was replaced with a flexible polymer@HPβCD-BTCA-based sheet. HPβCD-BTCA@PbI₂ complexes were

recovered either to be redissolved for active layer fabrication or to collect PbI₂ by dissolution in DI H₂O and centrifugation (Fig. 8c).

Another approach based on chemical coordination was reported by Ren *et al.*,⁷⁹ who employed zeolite to absorb Pb²⁺ ions. First, the HTL of the PSC was removed with ethyl acetate. Second, the perovskite active layer was dissolved in H₂O, where Pb²⁺ ions could be absorbed by the zeolite (with an adsorption efficiency of 100%), driving the ion exchange reaction (eqn (1)) towards the complete dissolution of PbI₂.



Finally, PbI₂ could be restored by the reaction of the I⁻-rich solution with Pb²⁺ ions desorbed from the zeolite. PSCs fabricated employing recycled PbI₂ displayed an even higher champion efficiency (21.58%) than pristine devices (21.50%). Hong *et al.*⁸⁰ compared the Pb²⁺ adsorption capacity of hydroxyapatite (HAP, Ca₁₀(PO₄)₆(OH)₂) with their synthesized whetlockite (WH, Ca₁₈Mg₂(HPO₄)₂(PO₄)₁₂), the first and second most abundant biominerals in human hard tissues, respectively. The results showed that WH had 1.68 times the absorption capacity of HAP, enabling 100% extraction of 3000 ppm of Pb²⁺ from a Pb(NO₃)₂ solution after 30 minutes. PbI₂ was then recovered by treating WH with absorbed Pb²⁺ with HNO₃ aqueous solution and KI. As-obtained recycled PbI₂ was tested for the fabrication of the active layer of PSCs, which attained an

average PCE of $19.0 \pm 1.4\%$, only slightly lower than the pristine PCE ($19.3 \pm 0.9\%$). Similarly, Park *et al.*⁸¹ synthesized an iron (Fe)-incorporated HAP (HAP/Fe) hollow composite to induce Pb^{2+} adsorption. After PSC dissolution in DMF, HAP/Fe composites were added to the solution, absorbing Pb^{2+} ions with a collection yield of 99.99%. The HAP/Fe@ Pb^{2+} complexes were removed from the solution by exploiting the magnetic properties induced by Fe incorporation by applying a magnetic field. PbI_2 was recrystallized by reaction with 1 M potassium iodide (KI) solution under acidic conditions, with a 99.97% recovery yield. Finally, PSCs were fabricated by employing recycled and commercial PbI_2 , which displayed average PCEs of $16.0 \pm 0.9\%$ and $16.6 \pm 1.0\%$, respectively.

Ultimately, Pb^{2+} can also be absorbed by organisms, such as fungi *Cladosporium* sp. strain F1, *A. niger* VKMF-1119 and *M. ramannianus* R-56, as demonstrated by Lee *et al.*⁸² Fungal strains were added to PbI_2 solutions in DI H_2O (pH 7), and their biosorption capacity was evaluated over time. *Cladosporium* sp. strain F1 exhibited the highest Pb^{2+} biosorption capacity, with a 94.1% extraction yield. PbI_2 was recovered with a 99.7% yield from the hyphae of *Cladosporium* sp. strain F1 by solvent treatment with DMSO in an acidic aqueous solution (pH 2) at 70 °C.

4.3.2. Recrystallization of lead iodide. A completely different environmentally friendly approach for PbI_2 recycling was adopted by Schmidt *et al.*,⁸³ who exploited the temperature dependence of PbI_2 solubility in H_2O . In fact, they used hot water to fully extract Pb from different perovskites, while cooling, they obtained pure solid PbI_2 . In detail, fragments (6–9 cm^2) of PSCs were immersed in H_2O at 50 °C for 62.5 minutes to induce perovskite degradation and PbI_2 dissolution. Subsequently, the solution was vacuum filtered to remove the solid components and cooled to 20 °C. At such a temperature, MAI, formamidinium iodide (FAI) and cesium iodide (CsI) are soluble in H_2O , while PbI_2 precipitates can be extracted from the solution (Fig. 9a). Employing this method, 97% of the PbI_2 contained in a PSC could be dissolved in H_2O , and $100 \pm 6\%$ of dissolved PbI_2 could be extracted from H_2O after two consecutive crystallization cycles (Fig. 9b). Therefore, the residue was metal-free and could be discarded as non-hazardous waste.

4.3.3. Electrochemical recycling of lead. Apart from absorption and recrystallization, electrochemistry can also be employed to recover Pb after perovskite dissolution. Wang *et al.*⁸⁵ utilized a lithium chloride (LiCl)–potassium chloride (KCl) eutectic composition, while Poll *et al.*⁸⁶ opted for choline chloride (ChCl):ethylene glycol (EG) = 1:2 deep eutectic solvent to dissolve the perovskite. In both cases, the yields of Pb^{2+} dissolution were very high, namely 99.9% and 99.7%, respectively. Recovery yields were only reported by Wang *et al.*,⁸⁵ who achieved 91.5% and 98.0% metal Pb deposition yields after the first and second electrolysis cycles, respectively.

4.3.4. In situ perovskite recycling. Finally, Chhillar *et al.*⁸⁷ and Xu *et al.*⁸⁴ reported an *in situ* recovery of degraded perovskite films by the deposition of the organic component (MAI in both cases), dissolved in IPA, onto the degraded films. In both works, the optical, morphological and structural properties of the reformed perovskite were assessed and compared

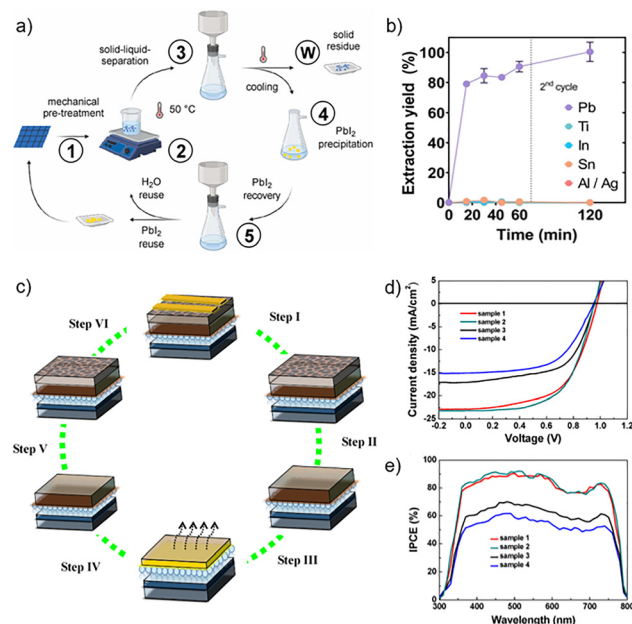


Fig. 9 (a) Scheme of the H_2O -based PbI_2 recycling process. The process includes mechanical fragmentation of PSCs (1), hot aqueous extraction (2), solid-liquid separation (filtration) (3), PbI_2 precipitation (cooling) (4) and recovery (5). PbI_2 can be reused in new perovskites. Solid waste (W) is deprived of Pb compounds. (b) Metal extraction from a PSC during two consecutive extraction cycles. Reproduced with permission.⁸³ Copyright 2023, Elsevier. (c) Schematic of *in situ* perovskite recycling from PSCs and sequential fabrication of new solar cells. (I) Removal of Ag electrode with adhesive tape. (II) Removal of the HTM by immersing in CB solvent. (III) Thermal decomposition of the perovskite into remained solid PbI_2 and emitted organic gases. (IV) Development of new perovskite films by spin coating a MAI solution. (V) Preparation of spiro-MeOTAD layer. (VI) Evaporation of Ag electrode. (d) J - V characteristics and (e) IPCE curves of PSCs fabricated with pristine PbI_2 (sample 1), recycled PbI_2 with optimized (sample 2) and non-optimized (sample 3) recycling procedure and second-time recycled PbI_2 (sample 4). Reproduced with permission.⁸⁴ Copyright 2017, Wiley.

to those displayed by fresh samples (Fig. 9c). Moreover, Xu *et al.*⁸⁴ tested the performance of devices fabricated with pristine and recovered perovskite films (Fig. 9d and e), which displayed 14.34% and 14.84% PCE, respectively, further demonstrating the efficacy of their recovery methods.

4.4. Recovery of multiple device components

To simultaneously overcome environmental and cost-related issues concerning PSCs, recovery strategies that simultaneously recycle and reuse more than one device component have been proposed. These processes are usually performed by sequentially dissolving each layer of the PSC stack, followed by specific treatments to recover each target material.

4.4.1. Simultaneous TCO/CTM reuse and PbI_2 recycling. Since TCO-coated substrates are the highest impacting components of PSCs and PbI_2 represents the most toxic compound of the device architecture, several recovery strategies combine TCO reuse with PbI_2 recycling. For instance, Chen *et al.*⁸⁸ developed a protocol based on perovskite dissolution and PbI_2 extraction, as presented in Fig. 10a.



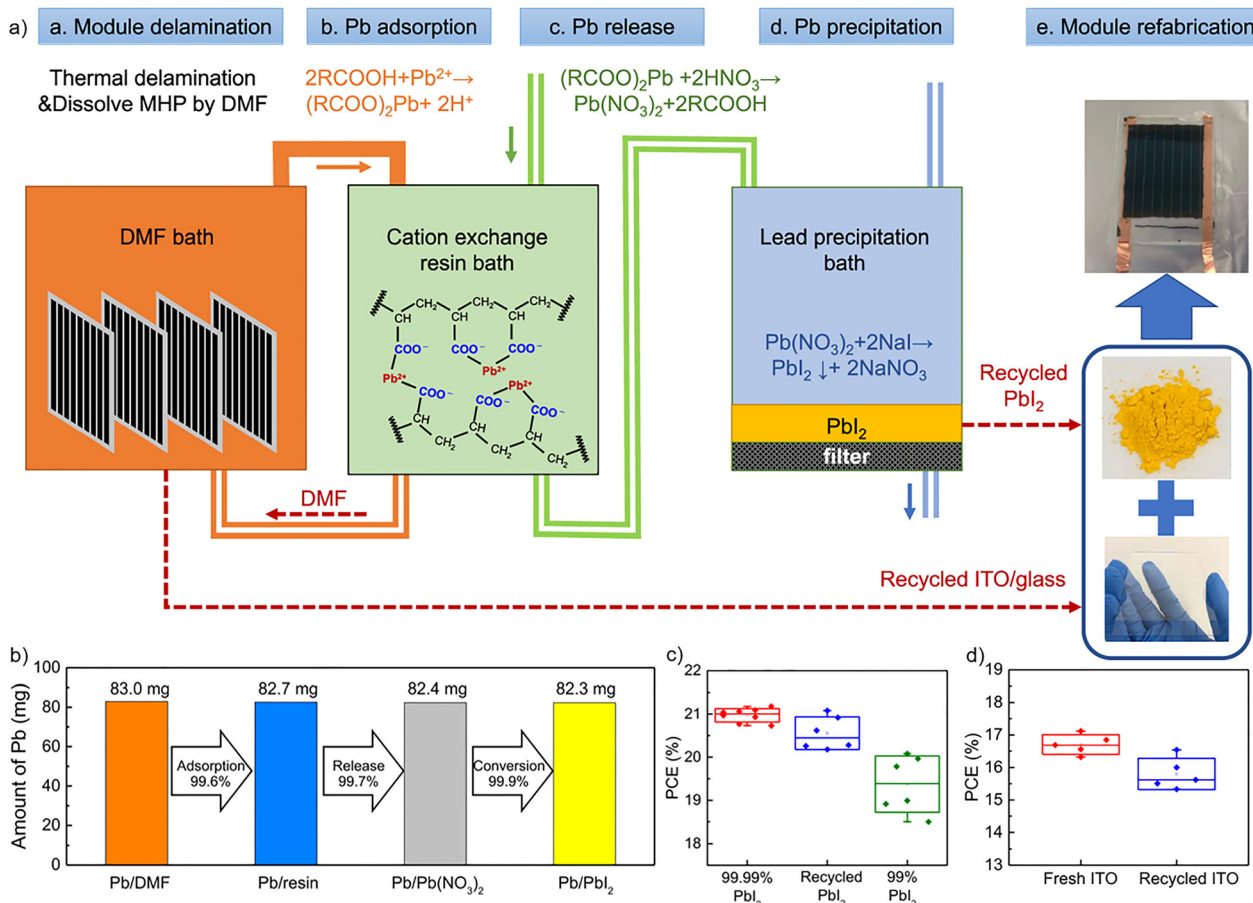
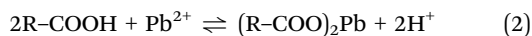


Fig. 10 (a) Scheme of PSM recycling: a. Encapsulated perovskite solar modules were delaminated, and the perovskite active layer was dissolved using DMF; b. Pb^{2+} was removed from DMF by carboxylic acid cation-exchange resin; c. Adsorbed Pb^{2+} ions on the resin were released to aqueous solution via resin regeneration process using HNO_3 ; d. PbI_2 was precipitated by pouring NaI into $\text{Pb}(\text{NO}_3)_2$ -containing solution; e. PSMs were refabricated employing recycled materials. (b) Pb^{2+} adsorption, release and conversion yields from 10 mL of 40 mM PbI_2 in DMF. (c) PCE box charts of PSCs (8 mm² device size) fabricated with commercial 99.99% PbI_2 , recycled PbI_2 , and commercial 99% PbI_2 . (d) PCE box charts of PSMs (25 cm² active area) fabricated on fresh and recycled ITO/glass. Reproduced with permission.⁸⁸ Copyright 2021, Nature.

First, the module encapsulation was removed by thermal delamination. Then, the ETL was washed with 1,2-dichlorobenzene, and PSMs were immersed in a DMF bath to dissolve the perovskite active layer. A carboxylic acid cation-exchange resin was employed to collect Pb^{2+} ions, exhibiting a 99.6% recovery yield (Fig. 10b). Pb^{2+} adsorption and release were governed by ion exchange between H^+ and Pb^{2+} ions, as described in the following equation:



Since eqn (2) describes a reversible reaction, the addition of H^+ ions could reverse the equilibrium towards Pb^{2+} release. Therefore, HNO_3 aqueous solution was used to release Pb^{2+} ions from the resin (with a 99.7% recovery yield, Fig. 10b), which were further treated with sodium iodide to precipitate PbI_2 (99.2% recovery yield). Recycled PbI_2 was employed to fabricate the active layer of new PSMs, which displayed a median of 20.4% PCE for 8 mm² devices, only 2.8% lower than the 21.0% PCE of pristine devices (Fig. 10c). Moreover, ITO/glass

and back cover glass were collected from PSMs and reused to fabricate 25 cm² active area modules. Devices produced with restored ITO/glass attained an average PCE of 15.9%, fairly similar to the average 16.7% PCE of pristine devices (Fig. 10d). Another approach was adopted by Deng *et al.*,⁸⁹ who dissolved the perovskite in DMF:DMSO = 9:1 and reused the resulting solution upon MAI addition to fabricate a recycled perovskite layer. Moreover, the same solvent composition was used to restore ITO/glass substrates. Champion PCEs of 16.6% and 15.3% were reported for devices produced with fresh and recycled materials, respectively. Zhang *et al.*⁹⁰ employed DMF to dissolve the perovskite active layer, displaying a dissolution yield of 99.9%. Then, the solution was treated with ammonia (NH_3) to precipitate lead hydroxide ($\text{Pb}(\text{OH})_2$), which was converted into PbI_2 by reaction with hydroiodic acid (HI). The resulting PbI_2 , obtained with a 95.7% reaction yield, displayed 99.9% purity. Morphological, optical and structural properties of both recycled PbI_2 and MAPbI_3 fabricated with recycled PbI_2 were assessed and compared with those displayed by fresh materials. Furthermore, PSCs produced using fresh and



recycled PbI_2 demonstrated similar PV performances, with 12.17% and 11.36% champion PCEs, respectively. Then, FTO/ $\text{c-TiO}_2/\text{m-TiO}_2$ substrates were recollected and structurally and optically compared to pristine substrates. PSCs fabricated with reused FTO/ $\text{c-TiO}_2/\text{m-TiO}_2$ displayed a 12.03% champion PCE, which is very close to the 12.21% champion PCE of fresh devices. Binek *et al.*⁹¹ achieved a 92–94% PbI_2 recovery yield by employing a dissolution-crystallization method. After the organic component (MAI) of the perovskite layer was removed with $\text{DI H}_2\text{O}$, PbI_2 was dissolved in DMF and extracted from the solvent under reduced pressure. The FTO/ TiO_2 substrates were further treated with DMF to completely remove the ETL. The effects of PbI_2 and FTO recycling on PSC performance were studied separately. Devices fabricated with fresh and recycled PbI_2 displayed 14.6% and 12.1% champion efficiencies, respectively. However, the use of recovered FTO glass substrates produced average PCEs of $13.4 \pm 1.1\%$, $12.8 \pm 1.3\%$ and $13.5 \pm 1.5\%$ for the 1st, 2nd and 3rd recovery iterations, respectively. Feng *et al.*⁹² treated the devices with a BA solution to dissolve the perovskite layer and the [6,6]-phenyl-C61-butyric acid methyl ester (PCBM) ETL. After BA evaporation, the solid precipitate was washed with toluene to remove PCBM and with ethanol to dissolve butylammonium iodide (BAI) and bathocuproine (BCP). Recycled MAPbI_3 crystals were then synthesized from recollected PbI_2 by employing a temperature-lowering method. Although fresh and recycled perovskite displayed very similar morphology and crystallinity, a red-shifted PL emission peak for recycled MAPbI_3 was attributed by the authors to the formation of shallow defects near the band edge. ITO/ NiO_x substrates were also refurbished and optically, morphologically and compositionally tested. Pristine and restored samples displayed similar properties, except for the presence of PbI_2 traces on the surface of the recovered ITO/ NiO_x . Nonetheless, the PV performances of the recovered devices were not negatively affected by PbI_2 residues. The recovered PSCs displayed a champion of 17.95% and an average of 17.27% PCE, which was even higher than the champion and average PCE of pristine devices, namely 17.84% and 17.18%, respectively.

4.5. Simultaneous TCO/ETL reuse and PbI_2 and HTL recycling

Utilizing approaches that simultaneously combine TCO and ETL reuse together with PSC multi-component recycling helps to alleviate pollution risks, decrease waste generation during the device recycling process, and lower EoL recycling costs. The recycling techniques discussed in this section focus on developing protocols for multiple material recovery. In the context of multiple-material recovery, the recycling of the top CTM of PSCs has also been included in several recovery strategies as an additional step in substrate reuse and PbI_2 recycling. Interestingly, all proposed processes are designed on the NIP and employ expensive spiro-OMeTAD as HTL.

Among these contributions, Wang *et al.*⁹³ demonstrated the recovery of ITO/ NiO_x substrates, the perovskite layer and the spiro-OMeTAD HTL using a “one-key bleacher” solution composed of methylamine and tetrahydrofuran (THF). Protocols

based on layer-by-layer schemes for disassembly require several steps to obtain proper material to reuse in refabricated PSCs, resulting in economically expensive protocols. In this work, the bleacher solution simultaneously dissolved the entire stack of the device, exposing the ITO/ NiO_x substrate (Fig. 11). Spiro-OMeTAD was recovered from THF by rotary evaporation, achieving 98.9% purity, and the methylamine solution containing the liquefied perovskite was utilised upon acetonitrile (ACN) addition to reform a perovskite layer with morphological and crystalline properties similar to those of fresh samples. PSCs fabricated with fresh and recycled components displayed similar performances, namely $20.6 \pm 0.6\%$ and $20.3 \pm 0.6\%$ respectively, and minimal PCE loss was displayed after repeating the recycling protocol two times ($20.1 \pm 0.6\%$ PCE). In a recent study, Wu *et al.*⁴⁵ demonstrated the recovery of ITO/ SnO_2 substrates, MAPbI_3 perovskite and spiro-OMeTAD HTL with almost 100%, 87% and 66% recovery yields, respectively. Spiro-OMeTAD was removed by dissolution in chlorobenzene (CB) and purified from its dopants through column chromatography. MAPbI_3 was then dissolved in γ -butyrolactone (GBL) and recrystallised with EtOH. Finally, additional SnO_2 deposition was performed onto recovered ITO/ SnO_2 substrates to improve the PV performances of recycled devices. After the comparison of fresh and recycled material properties, PSCs were fabricated by employing pristine and recovered components, demonstrating a champion 17.1% PCE, which is very similar to the champion 17.7% PCE of fresh devices. Additionally, the TCA and LCA of the proposed protocol were conducted, demonstrating the benefits of the adoption of such a recycling process with respect to a landfill EoL scenario. Similar results were demonstrated by our group⁴¹ for the recovery of ITO/ SnO_2 substrate, PbI_2 and spiro-OMeTAD, employing green solvents. Recycling yields were close to 100%, 99.4% and 89.2% for ITO/ SnO_2 , PbI_2 and spiro-OMeTAD, respectively. Spiro-OMeTAD was dissolved in EtOAc and purified from its dopants by MilliQ H_2O extraction. Formamidinium lead iodide (FAPbI_3) perovskite was removed from the ITO/ SnO_2 substrate by ultrasonication in $\text{DI H}_2\text{O}$, and PbI_2 was recrystallized with EtOH. Finally, ITO/ SnO_2 substrates were cleaned by sequential ultrasonication in the washing solution, $\text{DI H}_2\text{O}$, acetone and IPA. The properties of recovered materials were compared to those displayed by fresh components, and PSCs were fabricated to assess the impact of the recycling procedure on PV performance. Recycled PSCs displayed an average of 18.9% PCE, which is only 1.6% lower than the pristine average PCE (19.2%). The environmental advantages of the adoption of this recycling protocol with respect to a landfill EoL scenario were demonstrated by LCA. Moreover, the entire recovery protocol was repeated three times, and although PSCs displayed progressive PCE loss after each iteration, the energy return on investment (EROI) assessment revealed that the third iteration was still more convenient than landfilling. Finally, the solvents employed in the recycling protocol were recovered by distillation.

In summary, two major recycling methods for perovskite solar cells are generally applied. The first one, described in most of the procedures, involves the sequential dissolution of each single device layer (the layer-by-layer approach). Usually,



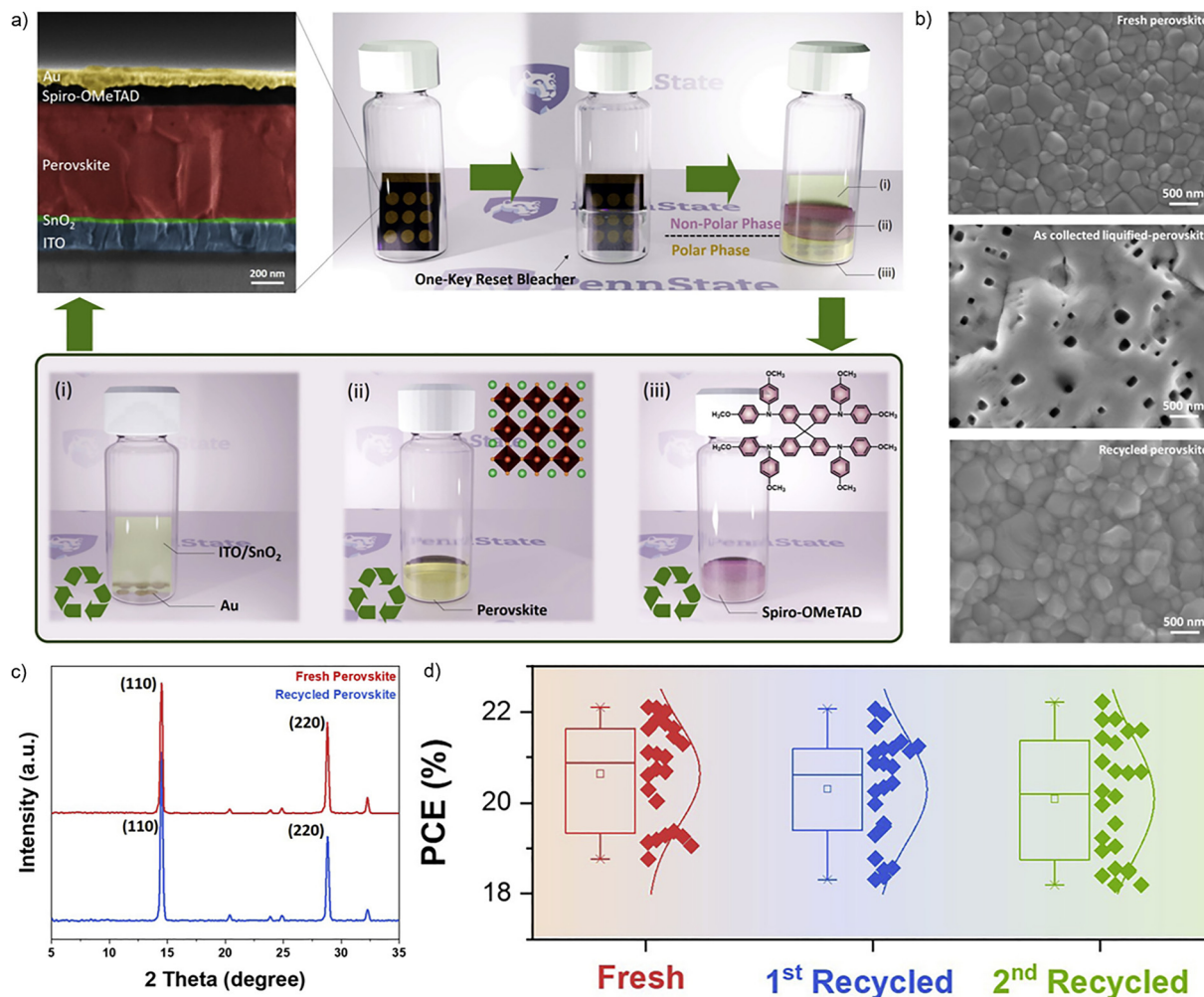


Fig. 11 (a) Cross section SEM image, showing the architecture adopted for PSCs, and schematic of how the bleacher solution simultaneously recycles multiple components: (i) Au and SnO₂-coated ITO/glass, (ii) liquified perovskite, and (iii) spiro-OMeTAD. (b) SEM images of fresh (top), liquified (middle) and recycled (bottom) perovskites. (c) XRD pattern of fresh and recycled perovskite films. (d) PCE box charts of PSCs fabricated with fresh and recycled components, with the recovery protocol iterated twice. Reproduced with permission.⁹³ Copyright 2021, Cell Press.

the top metal contact is typically removed through a tape-assisted lift-off process, followed by a series of sequential chemical treatments that enable the selective dissolution of the constituent layers of the device. The second method, less common, uses a “special” solution that can simultaneously dissolve the entire stack of the device in a single step. On the one hand, the layer-by-layer approach has been consolidated in several studies as an effective strategy for recycling methods for PSCs. On the other hand, the possibility of simultaneously recycling all components of perovskite-based devices in one step may represent a promising route to simplify the recycling complexity and reduce the LCOE of PSCs.

Importantly, it appears that the most virtuous PSC EoL management procedures (efficient in reducing energy requirements and environmental footprints) consider the use of “green solvents” or water-based solutions and exploit recycling protocols that allow recovering the most critical components of the device stack to reuse purified materials in multi-component

refabricated PSCs, lowering waste and costs in the EoL procedure. Additionally, in this case, the use of aqueous solutions or less toxic and environmentally friendly solvents is crucial for achieving efficient and sustainable decommissioning.

5. Importance of solvents (manipulation and or substitution towards green solvents)

As already mentioned, solvents significantly affect recovery techniques.⁴² The shift towards ecofriendly solvents represents a significant step towards real sustainability in PSC EoL. Therefore, this part of the review is dedicated to their selection. Specific criteria for their evaluation based on their impact on human health and the environment are first discussed. Finally, special attention is dedicated to their purification after use from a real circular economy perspective.



5.1. Criteria for solvent selection

First, a strategy that univocally identifies solvent hazards and environmental impacts must be defined. Several studies evaluate solvents based on combined LCA and environmental, health and safety (EHS) properties. Therefore, by coupling hazard estimations with full life-cycle resource exploitation and pollutant emissions, one can determine how green is a solvent.^{94,95} According to these guidelines, the Innovative Medicines Initiative (IMI)-CHEM21 public-private partnership consortium developed a solvent guide that combines the EHS criteria with LCA for common and bio-derived solvents, expanding the results previously reported by Prat *et al.*^{96,97} In their ranking, solvents are classified as recommended (or preferred), problematic, hazardous and highly hazardous based on the constraints that one should consider when employing them at the lab-scale or in a pilot line. Fig. 12a presents the IMI-CHEM21 ranking of solvents commonly employed for PSC manufacturing and recovery. Although only DMF is ranked as hazardous, owing to its high toxicity and environmental impact, many other common solvents, such as DMSO, THF and CB, are identified as problematic and are, therefore, not ideal to be employed in large-scale production. Among recommended solvents, we reported IMI-CHEM21 ranking of H₂O, EtOH, EtOAc, IPA and acetone, which were employed in some previously discussed recovery protocols. In this regard, Fig. 12b summarises the number of studies, among those analysed in the previous paragraphs, which report the use of a specific solvent as the main dissolution aid for the perovskite layer or CTMs and the impact of such solvent according to the IMI-CHEM21 ranking. Although several works adopted low-impact solvents, such as eutectic solvents, EtOH and H₂O, problematic solvents have been widely employed, and DMF was used in 15 of the mentioned publications. These results suggest that, although some efforts towards the use of safer solvents have been made, more awareness is needed when designing recovery

protocols, especially on solvent choice and solvent management. For example, in a very recent publication, Xiao *et al.*⁹⁸ showed that the development of a water-based solution is efficient for perovskite recycling. In the best closed-loop system scenario, the choice of using “green solvents” should also be considered from a fabrication viewpoint.^{30,99,100}

5.2. Solvent purification

Rodriguez-Garcia *et al.*⁴² estimated that solvent purification can significantly reduce the environmental impact of recovery processes by 56–68%. Moreover, from an economic viewpoint, Wu *et al.*⁴⁵ reported that by implementing solvent recycling into recovery strategies, the cost of PSMs fabricated with both refurbished materials and recycled solvents would be reduced by 18–20% with respect to the sole material reuse.

In a recent work from our group,⁴¹ we presented the purification of solvents employed in the recovery protocol with the aim of creating a process that could be as circular as possible. EtOAc, EtOH and DI H₂O were distilled, and their purification was evaluated with respect to specific contaminants, *i.e.* spiro-OMeTAD for EtOAc and PbI₂ for EtOH and DI H₂O, resulting in ~100%, 99.8% and 97.4% removal, respectively. Similarly, Kim *et al.*⁷⁰ reported that 99.99% of PbI₂ could be removed from the solvent used to dissolve the perovskite layer (DMF) by adsorption with HAP. In the context of DMF recovery, the use of such refurbished solvent to manufacture new PSCs was demonstrated by Kim *et al.*, who developed gelatine-conjugated hematite nanoparticles (HT NPs) that could effectively capture PbI₂ from both wastewater (even in binary systems, with 99.9% extraction efficiency).^{101,102} In the latter case, purified DMF was used, together with recovered spiro-OMeTAD dissolved in CB, to fabricate new PSCs, which exhibited an average $24.02 \pm 0.30\%$ PCE, very much similar to the $24.12 \pm 0.31\%$ PCE of devices produced with fresh solvents.¹⁰²

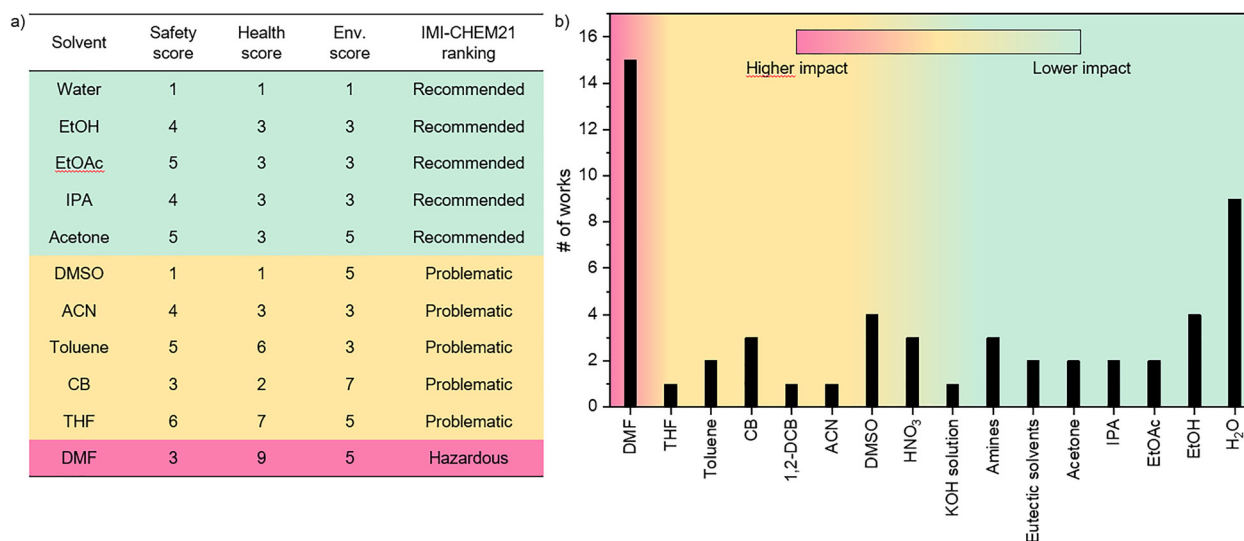


Fig. 12 (a) CHEM21 ranking of the solvents that are commonly employed to reuse and recycle critical components of PSCs. (b) Histogram presenting the number of works that report the use of several solvents for PSC recycling.



6. Conclusions and future perspectives

This review provided an important overview of the EoL management of depleted PSCs, which is a crucial issue that we encourage to take into consideration at the design stage, long before the commercialization of devices. In fact, since some PSC components are toxic, such as Pb and Pb-derived materials, inappropriate disposal of exhausted devices may lead to serious waste pollution, thus resulting in public environmental and health hazards.

Herein, we first presented the economic and environmental types of analysis that should be performed to assess the implications behind the recycling of PSCs. Such type of study is of fundamental importance to obtain a complete ETEA for evaluating PSC restoration, estimating both sustainability and economic advantages at once. As extensively demonstrated in the dedicated section of this review, TEA and LCA confirmed the economic benefits of developing recycling procedures that can reduce environmental impacts, both at the laboratory and industrial scales.

As TCO is the most impacting component, from both economic and environmental perspectives, extensive studies have been conducted to design its recovery. Overall, the reuse and restoration of TCO is a crucial step toward achieving a closed-loop system for perovskite solar cells, ensuring that these devices are both high-performing and environmentally friendly. Challenges in designing efficient close-looped strategies also come from the need to address the proper reuse of other impacting components, such as the encapsulation back glass and metal contacts.

Thus, following the waste hierarchy pyramid, aside from TCO/ETL reuse, it is also important to provide useful recycling protocols to simultaneously recover all materials composing the device stack, such as PbI_2 and HTL, to refabricate new high performance PSCs.

From a green chemistry perspective, we highlighted the major importance of solvent choice within recovery protocols, emphasizing the need for future studies to select solvents carefully based on their toxicity and environmental impact. Using “green solvents” should also be considered at the fabrication stage to achieve a total circular system.

In fact, designing recovery protocols that will be easily integrated into pilot lines and industrial manufacturing processes is fundamental to advancing towards PSC sustainable commercialization.

Furthermore, it is important to keep in mind different types of PSCs; for example, flexible devices that enlarge the field of application of perovskite-based PV technology. Since such devices employ alternative materials as substrates, it is urgent to plan new protocols for targeting proper recovery or recycling. In this respect, we envision new challenges in the recycling of flexible PSC substrates.

Finally, with the rapid advancement of the Internet of Things (IoT) in our society, the application of PSC as indoor photovoltaics (IPVs) can offer a promising solution to fulfil new

requests in terms of the type of energy font by providing lightweight power sources for IoT devices that can adapt to diverse indoor lighting conditions. In this respect, we foresee the rapid development of “*ad hoc*” and more and more virtuous sustainable and cost-efficient strategies to achieve proper EoL management integrated with a smart device design and environmentally friendly fabrication. This is essential to rapidly move from lab- to large-scale manufacturing in view of the forthcoming launch of perovskite-based PV technology to the market from a circular economy perspective.

Conflicts of interest

There are no conflicts to declare.

Data availability

All the presented data were extracted from previously published papers with the authors' obtained copyrights and processed using commonly available imaging software. Additional information is available from the corresponding author upon reasonable request.

Acknowledgements

This work was supported by FARE Ricerca in Italia Project (EXPRESS, no. R18ENKMTA3) and Fondazione Cariplo Economia Circolare 2021 Project (FLHYPER, no. 20201067). Authors acknowledge support from the GOPV project (CSEAA_00011), which received funds from Bando Ricerca di Sistema-CSEA-TIPO A Piano triennale 2019–2021 Decreto direttoriale 27 Ottobre 2021 del Ministero della Transizione Ecologica; MASE-(ex MITE); and Ministero dell'Università e della Ricerca and University of Pavia through the programme Dipartimenti di Eccellenza 2023–2027. Authors are grateful to Riccardo Pallotta for his precious support in the revision of the manuscript.

Notes and references

- 1 End of Life Management: Solar Photovoltaic Panels (IRENA, 2016).
- 2 H. Mirletz, H. Hieslmair, S. Ovaite, T. L. Curtis and T. M. Barnes, *Nat. Phys.*, 2023, **19**, 1376–1378.
- 3 V. Larini, L. Ardito, A. Messeni Petruzzelli, F. Matteucci and G. Grancini, *Chem*, 2023, **9**, 2738–2756.
- 4 M. A. Green, A. Ho-Baillie and H. J. Snaith, *Nat. Photonics*, 2014, **8**, 506–514.
- 5 National Renewable Energy Laboratory (NREL), Best Research-Cell Efficiency Chart.
- 6 S. D. Stranks, G. E. Eperon, G. Grancini, C. Menelaou, M. J. P. Alcocer, T. Leijtens, L. M. Herz, A. Petrozza and H. J. Snaith, *Science*, 2013, **342**, 341–344.
- 7 J. Y. Kim, J. W. Lee, H. S. Jung, H. Shin and N. G. Park, *Chem. Rev.*, 2020, **120**, 7867–7918.



- 8 C. Zuo, H. J. Bolink, H. Han, J. Huang, D. Cahen and L. Ding, *Adv. Sci.*, 2016, **3**, 1500324.
- 9 H. Zhu, S. Teale, M. N. Lintangpradipto, S. Mahesh, B. Chen, M. D. McGehee, E. H. Sargent and O. M. Bakr, *Nat. Rev. Mater.*, 2023, **8**, 569–586.
- 10 R. Pallotta, S. Cavalli, M. Degani and G. Grancini, *Small Struct.*, 2024, **5**, 2300448.
- 11 C. C. Boyd, R. Cheacharoen, T. Leijtens and M. D. McGehee, *Chem. Rev.*, 2019, **119**, 3418–3451.
- 12 B. Ding, Y. Ding, J. Peng, J. Romano-deGea, L. E. K. Frederiksen, H. Kanda, O. A. Syzgantseva, M. A. Syzgantseva, J. N. Audinot, J. Bour, S. Zhang, T. Wirtz, Z. Fei, P. Dörflinger, N. Shibayama, Y. Niu, S. Hu, S. Zhang, F. F. Tirani, Y. Liu, G. J. Yang, K. Brooks, L. Hu, S. Kinge, V. Dyakonov, X. Zhang, S. Dai, P. J. Dyson and M. K. Nazeeruddin, *Nature*, 2024, **628**, 299–305.
- 13 D. P. McMeekin, P. Holzhey, S. O. Furer, S. P. Harvey, L. T. Schelhas, J. M. Ball, S. Mahesh, S. Seo, N. Hawkins, J. Lu, M. B. Johnston, J. J. Berry, U. Bach and H. J. Snaith, *Nat. Mater.*, 2023, **22**, 73–83.
- 14 P. Mariani, M. Á. Molina-García, J. Barichello, M. I. Zappia, E. Magliano, L. A. Castriotta, L. Gabatel, S. B. Thorat, A. E. Del Rio Castillo, F. Drago, E. Leonardi, S. Pescetelli, L. Vesce, F. Di Giacomo, F. Matteocci, A. Agresti, N. De Giorgi, S. Bellani, A. Di Carlo and F. Bonaccorso, *Nat. Commun.*, 2024, **15**, 1–15.
- 15 S. P. Feng, Y. Cheng, H. L. Yip, Y. Zhong, P. W. K. Fong, G. Li, A. Ng, C. Chen, L. A. Castriotta, F. Matteocci, L. Vesce, D. Saranin, A. Di Carlo, P. Wang, J. Wei Ho, Y. Hou, F. Lin, A. G. Aberle, Z. Song, Y. Yan, X. Chen, Y. M. Yang, A. A. Syed, I. Ahmad, T. Leung, Y. Wang, J. Y. Lin, A. M. C. Ng, Y. Li, F. Ebadi, W. Tress, G. Richardson, C. Ge, H. Hu, M. Karimipour, F. Baumann, K. Tabah, C. Pereyra, S. R. Raga, H. Xie, M. Lira-Cantu, M. V. Khenkin, I. Visoly-Fisher, E. A. Katz, Y. Vaynzof, R. Vidal, G. Yu, H. Lin, S. Weng, S. Wang and A. B. Djurišić, *J. Phys. Mater.*, 2023, **6**, 032501.
- 16 European Commission, A new Circular Economy Action Plan For a cleaner and more competitive Europe, Brussels, 2020.
- 17 United Nations, Transforming our World: the 2030 Agenda for Sustainable Development, 2015.
- 18 X. Tian, S. D. Stranks and F. You, *Nat. Sustainability*, 2021, **4**, 821–829.
- 19 X. Tian, B. Roose, S. D. Stranks and F. You, *Energy Environ. Sci.*, 2023, **16**, 5551–5567.
- 20 G. Schileo and G. Grancini, *Lead or No Lead? Availability, Toxicity, Sustainability and Environmental Impact of Lead-Free Perovskites Solar Cells*.
- 21 V. K. Ravi, B. Mondal, V. V. Nawale and A. Nag, *ACS Omega*, 2020, **5**, 29631–29641.
- 22 T. Sanders, Y. Liu, V. Buchner and P. B. Tchounwou, Neurotoxic effects and biomarkers of lead exposure: a review, *Rev. Environ. Health*, 2009, **24**, 15–45.
- 23 F. Faini, V. Larini, A. Scardina and G. Grancini, *MRS Bull.*, 2024, **49**, 1059–1069.
- 24 C. C. Stoumpos, C. D. Malliakas and M. G. Kanatzidis, *Inorg. Chem.*, 2013, **52**, 9019–9038.
- 25 F. Wang, X. Zou, M. Xu, H. Wang, H. Wang, H. Guo, J. Guo, P. Wang, M. Peng, Z. Wang, Y. Wang, J. Miao, F. Chen, J. Wang, X. Chen, A. Pan, C. Shan, L. Liao and W. Hu, *Adv. Sci.*, 2021, **8**, 2100569.
- 26 X. Wu, B. Li, Z. Zhu, C. C. Chueh and A. K. Y. Jen, *Chem. Soc. Rev.*, 2021, **50**, 13090–13128.
- 27 R. Pallotta, M. Degani, F. Toniolo, S. Cavalli, F. Turci, W. Hua Bi, A. Girella, C. Milanese, A. Schöler, A. Magrez and G. Grancini, *Mater. Today Adv.*, 2024, **24**, 100541.
- 28 M. Degani, R. Pallotta, G. Pica, M. Karimipour, A. Mirabelli, K. Frohna, M. Anaya, T. Xu, C. Q. Ma, S. D. Stranks, M. L. Cantù and G. Grancini, *Adv. Energy Mater.*, 2025, **15**, 2404469.
- 29 R. Pallotta, F. Faini, F. Toniolo, V. Larini, M. Schmidt, S. Marras, G. Pica, S. Cavalli, S. Mattioni, L. E. Hueso, B. Martin-Garcia, B. Ehrler and G. Grancini, *Joule*, 2025, **9**(6), 101964.
- 30 C. Yang, W. Hu, J. Liu, C. Han, Q. Gao, A. Mei, Y. Zhou, F. Guo and H. Han, *Light: Sci. Appl.*, 2024, **13**, 227.
- 31 A. S. R. Bati, Y. L. Zhong, P. L. Burn, M. K. Nazeeruddin, P. E. Shaw and M. Batmunkh, *Commun. Mater.*, 2023, **4**, 2.
- 32 E. L. Unger, L. Kegelmann, K. Suchan, D. Sörell, L. Korte and S. Albrecht, *J. Mater. Chem. A*, 2017, **5**, 11401–11409.
- 33 F. U. Kosasih, E. Erdenebileg, N. Mathews, S. G. Mhaisalkar and A. Bruno, *Joule*, 2022, **6**, 2692–2734.
- 34 N. Bartie, L. Cobos-Becerra, F. Mathies, J. Dagar, E. Unger, M. Fröhling, M. A. Reuter and R. Schlattmann, *J. Ind. Ecol.*, 2023, **27**, 993–1007.
- 35 X. Wu, D. Zhang, X. Wang, X. Jiang, B. Liu, B. Li, Z. Li, D. Gao, C. Zhang, Y. Wang and Z. Zhu, *EcoMat*, 2023, **5**, e12352.
- 36 A. Maalouf, T. Okoroafor, Z. Jehl, V. Babu and S. Resalati, *Renewable Sustainable Energy Rev.*, 2023, **186**, 113652.
- 37 M. L. Parisi, S. Maranghi, L. Vesce, A. Sinicropi, A. Di Carlo and R. Basosi, *Renewable Sustainable Energy Rev.*, 2020, **121**, 109703.
- 38 M. De Bastiani, V. Larini, R. Montecucco and G. Grancini, *Energy Environ. Sci.*, 2022, **16**, 421–429.
- 39 A. Martulli, N. Rajagopalan, F. Gota, T. Meyer, U. W. Paetzold, S. Claes, A. Salone, J. Verboven, R. Malina, B. Vermang and S. Lizin, *Prog. Photovoltaics Res. Appl.*, 2023, **31**, 180–194.
- 40 Fraunhofer institute for solar energy systems ise. levelized cost of electricity renewable energy technologies June 2021.
- 41 V. Larini, C. Ding, B. Wang, R. Pallotta, F. Faini, L. Pancini, Z. Zhao, S. Cavalli, M. Degani, M. De Bastiani, F. Doria, C.-Q. Ma, F. You and G. Grancini, *EES Sol.*, 2025, DOI: [10.1039/D4EL00004H](https://doi.org/10.1039/D4EL00004H).
- 42 G. Rodriguez-Garcia, E. Aydin, S. De Wolf, B. Carlson, J. Kellar and I. Celik, *ACS Sustainable Chem. Eng.*, 2021, **9**, 15239–15248.
- 43 R. Vidal, J. A. Alberola-Borràs, S. N. Habisreutinger, J. L. Gimeno-Molina, D. T. Moore, T. H. Schloemer, I. Mora-Seró, J. J. Berry and J. M. Luther, *Nat. Sustainability*, 2021, **4**, 277–285.



- 44 European Chemical Agency (ECHA), Substance Infocard: N,N-dimethylformamide, <https://echa.europa.eu/substance-information/-/substanceinfo/100.000.617>, (accessed 24 July 2024).
- 45 Z. Wu, M. Sytnyk, J. Zhang, G. Babayeva, C. Kupfer, J. Hu, S. Arnold, J. Hauch, C. Brabec and I. M. Peters, *Energy Environ. Sci.*, 2024, **17**, 4248–4262.
- 46 L. McGovern, E. C. Garnett, S. Veenstra and B. van der Zwaan, *Sustainable Energy Fuels*, 2023, **7**, 5259–5270.
- 47 Y. Hu, T. Niu, Y. Liu, Y. Zhou, Y. Xia, C. Ran, Z. Wu, L. Song, P. Müller-Buschbaum, Y. Chen and W. Huang, *ACS Energy Lett.*, 2021, **6**, 2917–2943.
- 48 R. Deng, N. L. Chang, Z. Ouyang and C. M. Chong, *Renewable Sustainable Energy Rev.*, 2019, **109**, 532–550.
- 49 A. Binek, M. L. Petrus, N. Huber, H. Bristow, Y. Hu, T. Bein and P. Docampo, *ACS Appl. Mater. Interfaces*, 2016, **8**, 12881–12886.
- 50 European Parliament, Directive 2008/98/EC of the European Parliament and of the Council of 19 November 2008 on waste and repealing certain Directives (Text with EEA relevance), 2008.
- 51 P. Čulík, K. Brooks, C. Momblona, M. Adams, S. Kinge, F. Maréchal, P. J. Dyson and M. Khaja Nazeeruddin, Design and Cost Analysis of 100 MW Perovskite Solar Panel Manufacturing Process in Different Locations, *ACS Energy Lett.*, 2022, **7**, 3039–3044.
- 52 V. Larini, C. Ding, F. Faini, G. Pica, G. Bruni, L. Pancini, S. Cavalli, M. Manzi, M. Degani, R. Pallotta, M. De Bastiani, C. Q. Ma and G. Grancini, *Adv. Funct. Mater.*, 2023, 2306040.
- 53 B. L. Smith, M. Woodhouse, K. A. W. Horowitz, T. J. Silverman, J. Zuboy and R. M. Margolis, *Photovoltaic (PV) Module Technologies: 2020 Benchmark Costs and Technology Evolution Framework Results*, 2021.
- 54 L. McGovern, E. C. Garnett, S. Veenstra and B. van der Zwaan, *Sustainable Energy Fuels*, 2023, **7**, 5259–5270.
- 55 D. Bogachuk, P. van der Windt, L. Wagner, D. Martineau, S. Narbey, A. Verma, J. Lim, S. Zouhair, M. Kohlstädt, A. Hinsch, S. D. Stranks, U. Würfel and S. W. Glunz, *ACS Sustainable Resour. Manage.*, 2024, **1**, 417–426.
- 56 C. Zhang and N. G. Park, *Commun Mater.*, 2024, **5**, 194.
- 57 G. Li and H. Chen, *Sol. RRL*, 2024, **8**, 2400540.
- 58 E. S. Akulenko, M. Hadadian, A. Santasalo-Aarnio and K. Miettunen, *Heliyon*, 2023, **9**, e13584.
- 59 J. J. Cordell, M. Woodhouse and E. L. Warren, *Joule*, 2025, **9**, 101781.
- 60 C. Zhu, S. Li, Y. Li, K. Liu, J. Chen, B. Lu and X. Li, *Environ. Sci. Pollut. Res.*, 2023, **30**, 43472–43479.
- 61 Y. Zhu, Y. Kang, H. Huang, D. Zhuang, M. Li, Z. Ling, K. Peng, L. Zhai and C. Zou, *J. Mater. Chem. A*, 2023, **12**, 2916–2923.
- 62 H. Zhang, J. W. Lee, G. Nasti, R. Handy, A. Abate, M. Grätzel and N. G. Park, *Nature*, 2023, **617**, 687–695.
- 63 C. H. Chen, S. N. Cheng, L. Cheng, Z. K. Wang and L. S. Liao, *Adv. Energy Mater.*, 2023, **13**, 2204144.
- 64 M. M. Byranvand, W. Zuo, R. Imani, M. Pazoki and M. Saliba, *Chem. Sci.*, 2022, **13**, 6766–6781.
- 65 M. S. Chowdhury, K. S. Rahman, V. Selvanathan, A. K. M. Hasan, M. S. Jamal, N. A. Samsudin, M. Akhtaruzzaman, N. Amin and K. Techato, *RSC Adv.*, 2021, **11**, 14534–14541.
- 66 L. Huang, Z. Hu, J. Xu, X. Sun, Y. Du, J. Ni, H. Cai, J. Li and J. Zhang, *Sol. Energy Mater. Sol. Cells*, 2016, **152**, 118–124.
- 67 B. Augustine, K. Remes, G. S. Lorite, J. Varghese and T. Fabritius, *Sol. Energy Mater. Sol. Cells*, 2019, **194**, 74–82.
- 68 X. Feng, S. Wang, Q. Guo, Y. Zhu, J. Xiu, L. Huang, Z. Tang and Z. He, *J. Phys. Chem. Lett.*, 2021, **12**, 4735–4741.
- 69 W. Zhu, W. Chai, D. Chen, H. Xi, D. Chen, J. Chang, J. Zhang, C. Zhang and Y. Hao, *ACS Appl. Mater. Interfaces*, 2020, **12**, 4549–4557.
- 70 B. J. Kim, D. H. Kim, S. L. Kwon, S. Y. Park, Z. Li, K. Zhu and H. S. Jung, *Nat. Commun.*, 2016, **7**, 1–9.
- 71 L. Huang, J. Xu, X. Sun, R. Xu, Y. Du, J. Ni, H. Cai, J. Li, Z. Hu and J. Zhang, *ACS Sustainable Chem. Eng.*, 2017, **5**, 3261–3269.
- 72 X. Zhao, H. Shen, R. Sun, Q. Luo, X. Li, Y. Zhou, M. Tai, J. Li, Y. Gao, X. Li and H. Lin, *Sol. RRL*, 2018, **2**, 1700194.
- 73 Z. Ku, X. Xia, H. Shen, N. H. Tiep and H. J. Fan, *Nanoscale*, 2015, **7**, 13363–13368.
- 74 M. H. Li, Y. S. Yang, K. C. Wang, Y. H. Chiang, P. S. Shen, W. C. Lai, T. F. Guo and P. Chen, *ACS Appl. Mater. Interfaces*, 2017, **9**, 41845–41854.
- 75 D. Bogachuk, P. van der Windt, L. Wagner, D. Martineau, S. Narbey, A. Verma, J. Lim, S. Zouhair, M. Kohlstädt, A. Hinsch, S. D. Stranks, U. Würfel and S. W. Glunz, *ACS Sustainable Resour. Manage.*, 2024, **1**, 417–426.
- 76 J. M. Kadro, N. Pellet, F. Giordano, A. Ulianov, O. Müntener, J. Maier, M. Grätzel and A. Hagfeldt, *Energy Environ. Sci.*, 2016, **9**, 3172–3179.
- 77 G. Yang, M. Wang, C. Fei, H. Gu, Z. J. Yu, A. Alasfour, Z. C. Holman and J. Huang, *ACS Energy Lett.*, 2023, **8**, 1639–1644.
- 78 M. Yang, T. Tian, Y. Fang, W. G. Li, G. Liu, W. Feng, M. Xu and W. Q. Wu, *Nat. Sustainability*, 2023, **6**, 1455–1464.
- 79 M. Ren, Y. Miao, T. Zhang, Z. Qin, Y. Chen, N. Wei, X. Qian, T. Wang and Y. Zhao, *ACS Sustainable Chem. Eng.*, 2021, **9**, 16519–16525.
- 80 J. S. Hong, H. J. Kim, C. H. Sohn, O. Y. Gong, J. H. Choi, K. H. Cho, G. S. Han, K. T. Nam and H. S. Jung, *Energy Environ. Mater.*, 2023, **6**, 1–7.
- 81 S. Y. Park, J. S. Park, B. J. Kim, H. Lee, A. Walsh, K. Zhu, D. H. Kim and H. S. Jung, *Nat. Sustainability*, 2020, **3**, 1044–1051.
- 82 J. Lee, Y. Ko, S. Kim and H. G. Hur, *J. Hazard. Mater.*, 2023, **442**, 130106.
- 83 F. Schmidt, M. Amrein, S. Hedwig, M. Kober-Czerny, A. Paracchino, V. Holappa, R. Suhonen, A. Schäffer, E. C. Constable, H. J. Snaith and M. Lenz, *J. Hazard. Mater.*, 2023, **447**, 130829.
- 84 J. Xu, Z. Hu, L. Huang, X. Huang, X. Jia, J. Zhang, J. Zhang and Y. Zhu, *Prog. Photovoltaics Res. Appl.*, 2017, **25**, 1022–1033.
- 85 H. Wang, X. Chen, X. Li, J. Qu, H. Xie, S. Gao, D. Wang and H. Yin, *Chem. Eng. J.*, 2022, **447**, 137498.



- 86 C. G. Poll, G. W. Nelson, D. M. Pickup, A. V. Chadwick, D. J. Riley and D. J. Payne, *Green Chem.*, 2016, **18**, 2946–2955.
- 87 P. Chhillar, B. P. Dhamaniya, V. Dutta and S. K. Pathak, *ACS Omega*, 2019, **4**, 11880–11887.
- 88 B. Chen, C. Fei, S. Chen, H. Gu, X. Xiao and J. Huang, *Nat. Commun.*, 2021, **12**, 1–10.
- 89 F. Deng, S. Li, X. Sun, H. Li and X. Tao, *ACS Appl. Mater. Interfaces*, 2022, **14**, 52163–52172.
- 90 S. Zhang, L. Shen, M. Huang, Y. Yu, L. Lei, J. Shao, Q. Zhao, Z. Wu, J. Wang and S. Yang, *ACS Sustainability Chem. Eng.*, 2018, **6**, 7558–7564.
- 91 A. Binek, M. L. Petrus, N. Huber, H. Bristow, Y. Hu, T. Bein and P. Docampo, *ACS Appl. Mater. Interfaces*, 2016, **8**, 12881–12886.
- 92 X. Feng, Q. Guo, J. Xiu, Z. Ying, K. W. Ng, L. Huang, S. Wang, H. Pan, Z. Tang and Z. He, *Cell Rep. Phys. Sci.*, 2021, **2**, 1–15.
- 93 K. Wang, T. Ye, X. Huang, Y. Hou, J. Yoon, D. Yang, X. Hu, X. Jiang, C. Wu, G. Zhou and S. Priya, *Matter*, 2021, **4**, 2522–2541.
- 94 C. Capello, U. Fischer and K. Hungerbühler, *Green Chem.*, 2007, **9**, 927–993.
- 95 P. G. Jessop, *Green Chem.*, 2011, **13**, 1391–1398.
- 96 D. Prat, J. Hayler and A. Wells, *Green Chem.*, 2014, **16**, 4546–4551.
- 97 D. Prat, A. Wells, J. Hayler, H. Sneddon, C. R. McElroy, S. Abou-Shehadeh and P. J. Dunn, *Green Chem.*, 2015, **18**, 288–296.
- 98 X. Xiao, N. Xu and X. Tian, *et al.*, Aqueous-based recycling of perovskite photovoltaics, *Nature*, 2025, **638**, 670–675, DOI: [10.1038/s41586-024-08408-7](https://doi.org/10.1038/s41586-024-08408-7).
- 99 R. Vidal, J. A. Alberola-Borràs, S. N. Habisreutinger, J. L. Gimeno-Molina, D. T. Moore, T. H. Schloemer, I. Mora-Seró, J. J. Berry and J. M. Luther, *Nat. Sustainability*, 2021, **4**, 277–285.
- 100 H. J. Kim, Y. J. Kim, G. S. Han and H. S. Jung, Green Solvent Strategies toward Sustainable Perovskite Solar Cell Fabrication, *Sol. RRL*, 2024, **8**, 2300910, DOI: [10.1002/solr.202300910](https://doi.org/10.1002/solr.202300910).
- 101 H. J. Kim, J. M. Lee, J. H. Choi, D. H. Kim, G. S. Han and H. S. Jung, *J. Hazard. Mater.*, 2021, **416**, 125696.
- 102 H. J. Kim, O. Y. Gong, Y. J. Kim, G. W. Yoon, G. S. Han, H. Shin and H. S. Jung, *ACS Energy Lett.*, 2023, **8**, 4330–4337.

